ESTIMATING WATER STORAGE OF PRAIRIE POTHOLE WETLANDS

A Thesis Submitted to the College of

Graduate Studies and Research

In Partial Fulfillment of the Requirements

for the Degree of Master of Science

in the Department of Geography

University of Saskatchewan

Saskatoon

By

Adam George Nicholas Minke

PERMISSION TO USE

In presenting this thesis in partial fulfillment of the requirements for a postgraduate degree from the University of Saskatchewan, I agree that the Libraries of this University may make it freely available for inspection. I further agree that permission for copying of this thesis in any manner, in whole or in part, for scholarly purposes may be granted by the professor or professors who supervised my thesis work or, in their absence, by the Head of the Department or the Dean of the College in which my thesis work was done. It is understood that any copying or publication or use of this thesis or parts thereof for financial gain shall not be allowed without my written permission. It is also understood that due recognition shall be given to me and to the University of Saskatchewan in any scholarly use which may be made of any material in my thesis.

DISCLAIMER

Reference in this thesis to any specific commercial products, process, or service by trade name, trademark, manufacturer, or otherwise, does not constitute or imply its endorsement, recommendation, or favouring by the University of Saskatchewan. The views and opinions of the author expressed herein do not state or reflect those of the University of Saskatchewan, and shall not be used for advertising or product endorsement purposes.

Requests for permission to copy or to make other uses of materials in this thesis in whole or part should be addressed to:

Head of the Department of Geography
Department of Geography
Room 125 Kirk Hall
117 Science Place
University of Saskatchewan
Saskatoon, Saskatchewan
S7N 5C8
Canada

ABSTRACT

The Prairie Pothole Region (PPR) of North American contains millions of wetlands in shallow depressions that provide important hydrological and ecological functions. To assess and model these functions it is important to have accurate methods to quantify wetland water volume storage. Hayashi and van der Kamp (2000) developed equations suitable for calculating water volume in natural, regularly shaped wetlands when two coefficients are known. This thesis tested the robustness of their full and simplified volume (*V*) area (*A*) depth (*h*) methods to accurately estimate volume for the range of wetland shapes occurring across the PPR. Further, a digital elevation model (DEM) derived from light detection and ranging (LiDAR) data was used to extract the necessary data for applying the simplified *V-A-h* method at a broad spatial scale. Detailed topographic data were collected for 27 wetlands in the Smith Creek Research Basin and St. Denis National Wildlife Area, Saskatchewan that ranged in surface area shape. The full *V-A-h* method was found to accurately estimate volume (errors ≤5%) across wetlands of various shapes and is therefore suitable for calculating water storage in the variety of wetland shapes found in the PPR. Analysis of the simplified *V-A-h* method showed that the depression (*p*) and size (*s*) coefficients are sensitive to the timing of area and depth measurements and the accuracy of area measurements. Surface area and depth should be measured concurrently at two points in time to achieve volume errors <10%. For most wetlands this means measuring area and depth in spring when water levels are ~70% of h_{max}, and also in late summer prior to water depths dropping below 0.1 m. The wetted perimeter of the deepest water level must also be measured accurately to have volume errors less than 10%. Applying the simplified *V-A-h* method to a LiDAR DEM required GIS analysis to extract elevation contours that represent potential water surfaces. From these data the total wetland depth and *s* coefficient were estimated. Volume estimates through this

LiDAR *V-A-h* method outperformed estimates from two volume-area equations commonly used in the PPR. Furthermore, the process to extract the wetland coefficients from the LiDAR DEM was automated such that storage could be estimated for the entire St. Denis National Wildlife Area. Applying the simplified *V-A-h* method according to the guidelines and data sources recommended here will allow for more accurate, time-effective water storage estimates at multiple spatial scales, thereby facilitating evaluation and modelling of hydrological and ecological functions.

ACKNOWLEDGEMENTS

I am grateful to Masaki Hayashi, Garth van der Kamp, and Randy Schmidt for providing bathymetric data for SDNWA. I would like to thank Nathalie Brunet, Logan Fang, and Larisa Barber for collecting the survey data for SCRB, and the residents of SCRB for permission to access their land. I am grateful to John Pomeroy, Kevin Shook, Garth van der Kamp, Bob Clark, and Juxin Liu for their insights and suggestions. I would like to acknowledge Cherie for her guidance over the last two years. She has been instrumental in helping me develop my knowledge of hydrology, my ability to undertake research, and my confidence. This research was supported by grants from the Prairie Farm Rehabilitation Association, Manitoba Habitat Heritage Corporation, and Prairie Provinces Water Board (PPWB). A monthly salary was possible because of the Alexander Graham Bell Canada Graduate Scholarship-Masters (CGSM) that was awarded by the Natural Science and Engineering Research Council of Canada (NSERC), and the Dean's Scholarship that was awarded by the University of Saskatchewan. I would like to thank the Saskatchewan Watershed Authority and PPWB for processing and providing the LiDAR DEM. I am also grateful to Malcolm Conly for his efforts in acquiring the LiDAR data for SDNWA. I would also like to thank Ducks Unlimited Canada, Dan Pennock, and Mark Bidwell for their donation of an extensive collection of remote sensing and GIS data for SCRB and SDNWA.

I would like to thank my Dad, Mum, and Brother for always supporting and encouraging me. They were there for me when times were difficult and I am forever grateful for them. I am thankful for all of my friends, both those attending the university and those who aren't. They have been there to listen, laugh and dance with, which thankfully took my mind off school. Lastly, I am grateful that God has placed me here and that He has cared for me during the last two years. Everything I am is because of Him.

TABLE OF CONTENTS

LIST OF TABLES

LIST OF FIGURES

LIST OF ABBREVIATIONS

A	surface area of water (m^2 unless otherwise specified)
A_{DEM}	area measured from the topographic survey-derived DEM
A_{err}	the RMS area error (%)
Δh	change in depth of water (m)
DEM	Digital Elevation Model
GCP	Ground Control Point
h	depth of water above the bottom of the wetland (m)
h_{min}	the lowest point in the wetland (m)
h_{max}	the maximum depth of water in the wetland (m)
h_o	the unit of depth measurement (m)
km	kilometre
LiDAR	Light Detection and Ranging
m	metres
mm	millimetres
n	number of data points for RMS error
p	the Hayashi-van der Kamp wetland basin coefficient
P	perimeter
P	statistical significance value
PPR	Prairie Pothole Region
r^2	coefficient of determination
R.M.	Rural Municipality
RMS	Root-Mean-Squared [error] (%)
s	the Hayashi-van der Kamp wetland shape coefficient
SCRB	Smith Creek Research Basin
SDNWA	St. Denis National Wildlife Area
SI	Shape Index
V	volume of water (m^3 unless otherwise specified)
V-A-h	the Hayashi-van der Kamp volume-area-depth relationship
V_{DEM}	volume measured from the topographic survey-derived DEM
V_{err}	the RMS volume error (%)

CHAPTER 1 – INTRODUCTION

1.1. Prairie Pothole Region

The Prairie Pothole Region (PPR) of North America (Figure 1.1) is a vast area (~780,000 km^2) that contains between 5 and 60 wetlands per km^2 (National Wetlands Working Group 1988). These wetlands, commonly termed potholes, provide important hydrological and ecological functions, such as supporting more than half of North American waterfowl (Ogaard et al. 1981, Johnson et al. 2005), acting as a sink for agricultural-derived nutrients (van der Valk 1989, Whigham and Jordan 2003), and storing surface water which can attenuate flood flows (Hubbard and Linder 1986, Gleason and Tangen 2008).

Figure 1.1. Prairie Pothole Region of North America

Wetlands are recognized by certain physical and biological characteristics, such as having standing water, hydric soil conditions, and vegetation adapted to wet conditions (Mitsch and

Gosselink 1993). According to the Canadian wetland classification there are two types of wetlands found in the PPR, marsh wetlands and shallow water wetlands (Warner and Rubec 1997). Marshes are characterized by standing or slow moving water, mineralized soils and emergent vegetation, such as reeds. Shallow water wetlands are not commonly part of a river system, have shallow water levels and are in the stage between marshes and lakes. Further definition of prairie pothole wetlands can be found within the hydrogeomorphic classification developed by Brinson (1993). According to the geomorphic setting, Brinson (1993) described pothole wetlands as topographic depressions primarily having no permanent inlet or outlet. This is due to the last glaciation which shaped the topography of the landscape. The abrasion from glacier movement levelled the land surface, depositing fine silts and clays (Huel 2000). Once the glaciers retreated there were millions of large ice chunks left buried in the soil. When this ice melted the soil subsided, which created small depressions that are now prairie pothole wetlands (Huel 2000). Since the topography is so flat and without a developed drainage network, many of these wetlands are in areas that do not contribute to streamflow, termed non-contributing areas or gross drainage areas (Goodwin and Martin 1975, Winter et al. 1984). However, in years where high precipitation has maximized water storage or when land use practices have artificially created surface connections to the stream channels, normally isolated wetlands may contribute to streamflow (Stichling and Blackwell 1957). Artificially draining wetlands removes water that would normally stay on the land and contributes it to streamflow. Since the settlement of the prairies approximately 70% of the wetlands have been removed (Schindler and Donahue 2006). The impact on prairie hydrology is not fully understood because we currently do not have accurate estimates of wetland water storage at the landscape scale. Knowing the quantity of water stored in these wetlands would allow for a better assessment of wetland functions and

improved accuracy of hydrological models that predict the water balance, including streamflow, for watersheds within the PPR (Fang and Pomeroy 2007).

1.2. Prairie Hydrology

The prairie region is characterized by cold, long winters with approximately 30% of total annual precipitation falling as snow (Pomeroy et al. 2007). Summer precipitation is a result of short duration, intense convective storms with limited spatial extent. The infiltration capacity of the soils during the summer is very high which allows nearly all precipitation to be infiltrated (Elliot and Efetha 1999). Consequently, minimal surface runoff is produced during these rain events (Hayashi et al. 1998). Snowfall is spatially homogeneous across the landscape; however, blowing snow is responsible for redistributing snow across large areas and into wetlands (LaBaugh et al. 1998). Wetlands act as a sink for blowing snow due to exposed vegetation around the perimeter and their low topographic position in the landscape (Winter and Rosenberry 1995, van der Kamp et al. 2003, Fang and Pomeroy 2008). This effect is especially enhanced when surrounding agricultural land is fallow (Pomeroy and Gray 1995). When the trapped snow melts in spring, it provides the majority of water that fills pothole wetlands (Fang and Pomeroy 2008).

Melting snow in the spring causes significant surface runoff. During the initial stages of snowmelt, water is transported over frozen soil which restricts infiltration capacity (Gray et al. 1985, Winter and Rosenberry 1995). Runoff water collects in topographic depressions that contain wetlands. Later in the snowmelt period the land cover and soil infiltration plays an important role in the quantity of surface runoff reaching the wetland. With permanent grass surrounding the wetland the macropore network increases infiltration and results in water lost to

the root zone instead of recharging wetland water levels (van der Kamp et al. 2003). When snowmelt is exhausted the water levels of prairie pothole wetlands will fluctuate mainly due to evapotranspiration, and to a lesser extent, groundwater interaction.

Wetlands have a dynamic relationship with groundwater. In many cases the primary hydrologic cause for wetland formation is the interception of the local water table with the surface (Warner and Rubec 1997). This results in many wetlands being a recharge zone for groundwater. Wetlands of the PPR are unique in being situated on low permeability glacial tills. This till layer negates groundwater interaction in the uplands and restricts wetlands from recharging regional flow systems (Winter and Rosenberry 1995). However, recharge to local groundwater flow is common and is important to groundwater supplies (van der Kamp and Hayashi 1998). Groundwater recharge is 2-40 mm per year, with the majority occurring through fractures and preferential flow paths (van der Kamp and Hayashi 1998). This recharge rate is relatively low when compared to gravel or sand substrates, which could be eight orders of magnitude greater (Winter and LaBaugh 2003). Hayashi et al. (1998) estimated that only ~1 to 8% of the water lost annually from a prairie pothole wetland goes towards recharging the groundwater aquifer. Therefore, groundwater recharge has a minor influence on wetland water level drawdown in the PPR. The dominant cause of water level drawdown is evapotranspiration. This is the combined effect of transpiring vegetation and open water evaporation. Transpiration is common in prairie pothole wetlands that have a ring of phreatophytic vegetation, such as willow or poplar surrounding the water (Meyboom 1966). Photosynthetically active vegetation will pull water laterally from the wetland during summer months and transpire it to the atmosphere (Millar 1971). As much as 70% of water that infiltrates under wetlands moves to local riparian vegetation and is transpired (Parsons et al. 2004). When a ring of phreatophytic

vegetation is not present, such as when agricultural lands are left fallow, transpiration rates are reduced (Hayashi et al. 1998). In this situation evaporation directly from the water surface is the dominant loss of water from the wetland. The combined losses from evaporation and transpiration have been found to be between 3-5 mm of water loss per day (Rosenberry and Winter 1997, Parkhurst et al. 1998). This amount of water loss can be approximately double the summer precipitation (Price 1993, Parkhurst et al. 1998). As a result, water levels gradually decline during the summer for many pothole wetlands. Large wetlands tend to exhibit a slower loss of water though the summer. The difference is due to the larger heat storage capacity and lower area/shoreline ratio of larger wetlands, resulting in less loss to transpiring vegetation (Millar 1971, Parkhurst et al. 1998).

1.3. Water Storage Estimation Methods for Prairie Pothole Wetlands

The water level fluctuation of wetlands in the PPR is dynamic, with a large amount of seasonal variability (van der Valk 2005). This water level fluctuation makes it difficult to generalize water storage characteristics across a prairie watershed. Therefore, it is critical to use accurate methods to quantify water storage volumes in order to assess ecological and hydrological functions. Currently, there are many methods available to estimate wetland storage in the PPR, each having a specific accuracy, data requirement, or applicable scale.

Due to the vast number of wetlands in the PPR it is difficult to quantify the amount of water volume stored in every depression. As a result, storage information is primarily calculated for large water bodies, such as lakes or wetlands in a specific, small area. A simple method for estimating volume involves multiplying the average depth of a water body by the area (Taube 2000). This method is advantageous due to the simplicity of the mathematics; however, it does

not incorporate basin morphology and leads to relatively inaccurate estimates of volume (Taube 2000). When accurate calculations of volume are required it is necessary to collect detailed topographic data. For example, to understand certain wetland functions, such as vegetation composition or water chemistry, it is necessary to accurately characterize the depth-volume relationship (Woo and Rowsell 1993, Poiani et al. 1996, Waiser 2006, Voldseth et al. 2007). Depth-volume relationships require a detailed topographic survey of the study wetland to derive a regression equation that will estimate volume based on water depth. While this approach is useful for the individual wetland, the equations are time consuming to produce and lack transferability to other locations. Since there is a strong statistical relationship between volume (V), area (A), and the depth of water (h) in a topographic depression (Haan and Johnson 1967, Ullah and Dickinson 1979), a general equation relating the three variables would assist in estimating the water volumes stored in prairie pothole wetlands. Hayashi and van der Kamp (2000) investigated the *A-h* and *V-h* relationships of wetlands in three PPR sites to develop a simple power equation that can estimate wetland volume based on the depression profile (p coefficient) and size of the wetland (s coefficient). The p coefficient is an important feature of the *V-A-h* relationship because it incorporates depression morphology when estimating wetland volume. This method provides accurate volume and area estimations when detailed survey data are available, and has since been used to model depth-volume relationships for individual or small groups of wetlands in selected areas of the PPR (Hayashi et al. 2003, Carroll et al. 2005, Hill et al. 2006, Waiser 2006). When a detailed topographic survey is not available, the *V-A-h* coefficients can be derived through a less data intensive method (Hayashi and van der Kamp 2000), hereafter termed the simplified *V-A-h* method, which requires concurrent measures of surface area and depth at two points in time, provided that Δh and $\Delta A > 0$. Because area and

depth measurements could easily be collected for many wetlands, and volumes could be estimated with limited time invested.

It is clear from the above discussion that methods are available to quantify water volume for specific, small areas with detailed topographic information. However, hydrologists are constantly trying to improve predictions for larger areas while using limited data. The use of aerial photography has enabled researchers to estimate wetland water storage for large scales (e.g., >1,000 hectares) (Ludden et al. 1983). These methods use black and white photography to derive contours maps (~0.3 m contours) that allow area and depth to be calculated. By using a geometric shape, such as a cone, to approximate the basin, volume can be calculated for each contour with

$$V = \frac{1}{3} H\left(A_1 + A_2 + \sqrt{(A_1 \times A_2)}\right) \qquad (1.1)$$

where H is the difference in depth between two contours, A_1 is the area of the upper contour and A_2 is the area of the lower contour (Ludden et al. 1983, Taube 2000). This method involves calculating volume for each contour interval, then summing the results to get a volume for the entire depression. When storage capacity had been calculated for a number of sites, the results can be extrapolated to quantity the amount of water stored in a watershed (Ludden et al. 1983, Hubbard and Linder 1986). This method allows for a relatively accurate calculation of water storage but also requires an immense amount of time to create contour maps and calculate volume for each contour. Although this method is not commonly used, aerial photography has been collected since the mid-twentieth century and can be used to derive area extents of wetlands (Conly and van der Kamp, 2001). Considering the strong relationship between area and volume

(Haan and Johnson 1967), attempts have been made to estimate wetland volume from wetland area alone. Volume-area (*V-A*) relationships are commonly used because storage can be easily estimated for large areas. This method involves field surveying a sample of wetlands to derive a regression equation that statistically relates area to volume and then using the relationship along with remote sensing-derived area measurements to estimate volume at the watershed scale (Haan and Johnson 1967, Wiens 2001, Gleason et al. 2007). Wiens (2001) had to analyze the *V-A* relationship of 170 wetlands in order to derive his regression equations. For these wetlands, Wiens developed two regression formulae to account for the different *V-A* relationship observed between small (<70 ha) and large (>70 ha) wetlands. Gleason et al. (2007) suggested the *V-A* method could be improved by developing unique *V-A* relationships for the three main physiographic regions in the PPR. This is because variation in topographic relief causes a wide range of wetland morphologies with different *V-A* relationships (Gleason et al. 2007). While *V-A* relationships have been used for large scale investigations of water storage, there is concern they do not provide accurate estimates of volume. For example, Wiens (2001) concluded that the *V-A* approach is primarily useful for calculating wetland water storage for an entire watershed and is extremely limited for estimating individual wetland volumes. This is because the *V-A* method does not use a measurement of wetland depth to account for variation in basin morphology.

The Digital Elevation Model (DEM) is a data source that has a large spatial extent and can provide information on wetland characteristics, such as area and depth. DEMs are essentially a grid of elevation values. Traditional GIS analysis, such as "filling" the depressions, artificially raises the elevation value of the depression to the elevation of the surrounding cell (Jenson and Domingue 1988). While the intention of this analysis is to remove impedances to flow, the original DEM can be subtracted from the 'filled' DEM to give a measure of the depression depth

(Martz and De Jong 1988). This method can be easily implemented in a GIS to extract wetland depth and surface area information from depressions in the DEM (Martz and de Jong 1988, Vinning 2002, Gusman et al. 2004, Wang et al. 2008). However, readily available DEM data are coarse (10-20 meters) and this method often generalizes depression characteristics when calculating volume. Current DEM analysis would benefit from integrating a parameter, such as the *p* coefficient from the Hayashi-van der Kamp *V-A-h* equations to account for depression morphology. Recent advances in data acquisition through light detection and ranging (LiDAR) have provided DEMs with sub-meter spatial resolution and vertical accuracy. With LiDAR-derived DEMs it is possible to collect high resolution topographic data for depressions (Lindsay and Creed 2004, Liu and Wang 2008) and wetlands (Töyrä et al. 2003). Therefore, it could be possible to collect area and depth measurements of sufficient accuracy that wetland volume could be estimated through the simplified *V-A-h* method.

1.4. Objectives

It is important to have simple, accurate methods to estimate wetland storage in the Prairie Pothole Region (PPR) to assess wetland functions such as nutrient cycling, habitat availability, and runoff generation in natural and altered watersheds. Hayashi and van der Kamp (2000) utilized the strong statistical relationship between volume, area, and depth to develop two equations for estimating wetland volume and area based on the depression profile (*p* coefficient) and size (*s* coefficient) of the wetland. Since their method was tested only on regularly shaped, natural wetlands, there is a need to ensure that the *V-A-h* equation can reliably estimate volume for the broad range of wetland morphologies observed across the PPR. Hayashi and van der Kamp also recommended a simplified *V-A-h* method that could be applied with limited

topographic data, such as when only two concurrent measures of *A* and *h* are known. However, they did not report guidelines for using the method or a detailed report of the results. Within this context, my first objective was to:

1a) Determine how variation in wetland surface area shape influences estimates of water storage volumes through the Hayashi-van der Kamp *V-A-h* method.

1b) Develop guidelines for applying the simplified *V-A-h* method to wetlands throughout the PPR.

Since there is a lack of widely available detailed topographic information, such as survey or depth data, the full *V-A-h* method has only been applied at the individual wetland scale. However, the simplified *V-A-h* method holds much potential for estimating water storage at a greater spatial scale because only limited topographic data are required. Since high resolution LiDAR data can be acquired for large areas, there is promise that the simplified *V-A-h* method may be used to estimate wetland water storage at the catchment scale. Within this context, my second objective was to:

2a) Evaluate whether the Hayashi-van der Kamp coefficients can be derived from a LiDAR DEM and used in the simplified *V-A-h* method to estimate the volume of water stored in individual wetlands.

2b) Determine if the process to retrieve the coefficients from a LiDAR DEM can be automated such that wetland water storage could be estimated at a greater spatial scale.

CHAPTER 2 – METHODS

2.1. Study Sites

2.1.1 Smith Creek Research Basin

One of the study sites was the Smith Creek Research Basin (SCRB). SCRB is located in east-central Saskatchewan (101° 47’ W and 51° 00’ N) in the R.M. of Churchbridge and Langenburg (Figure 2.1). This site is being investigated as part of a larger study aimed at developing a hydrological model that will better predict runoff in prairie watersheds.

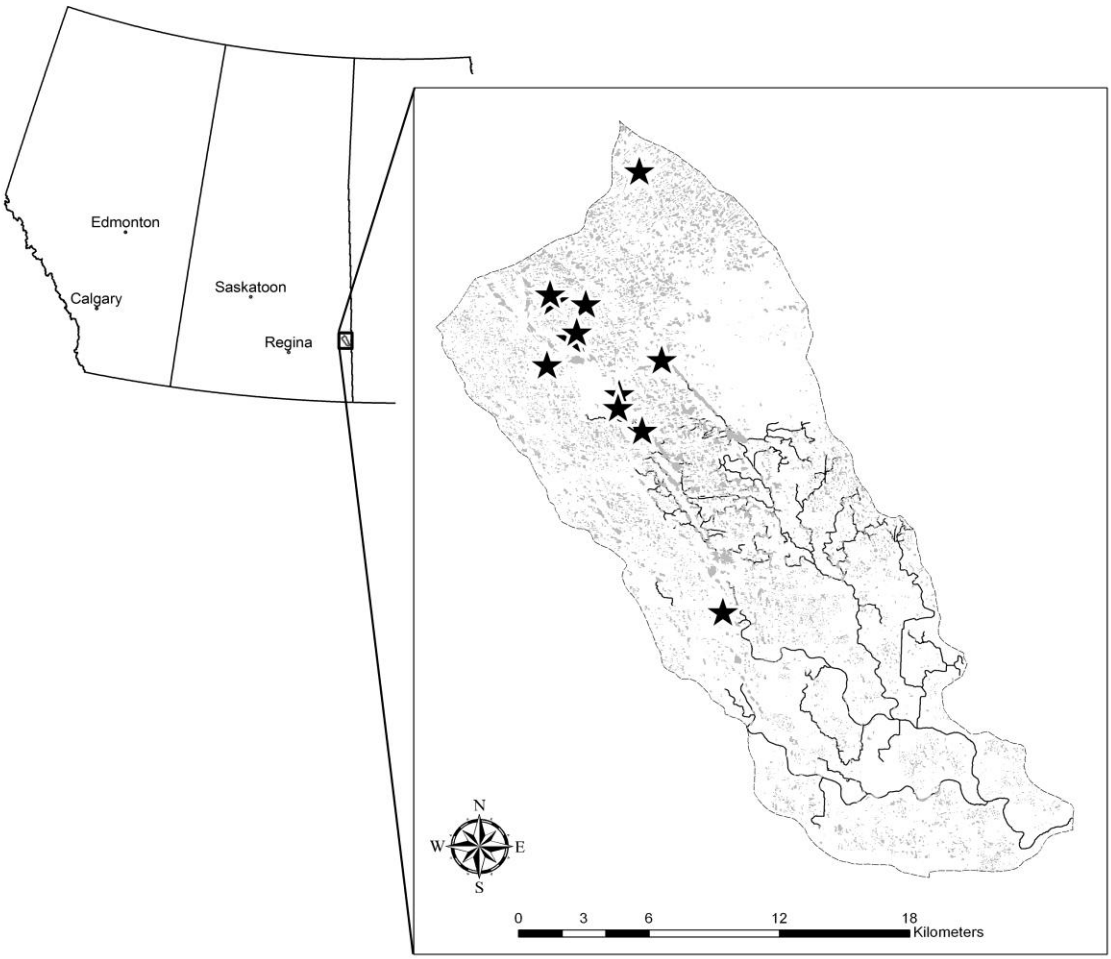

Figure 2.1. Map of Smith Creek Research Basin (SCRB) depicting the extent of wetlands in the basin as of 2000 (grey shading), as well as Smith Creek (line network) and wetlands with survey data (stars).

SCRB is within the PPR and has an abundance of wetlands. The watershed is ~445 km^2 and has an effective contributing area of 85 km^2, as measured by the Prairie Farm Rehabilitation Association (PFRA 2008). The topography is relatively flat, with slopes of 1-5%. Agriculture is the dominant land-use in the basin, occupying ~48% of the watershed. In recent years, agricultural drainage has removed many of the wetlands from the landscape. In 1958, wetlands accounted for ~17% of the land-cover in the basin, whereas in 2007 wetlands accounted for ~8%. The majority of wetlands in SCRB can be classified as isolated basin marshes. These wetlands are situated in shallow topographic depressions and have dramatic water level fluctuations (Warner and Rubec, 1997). According to the wetland geomorphic classification (Brinson, 1993), SCRB wetlands may also be called depressional wetlands. Most have no apparent natural outlet and lose water primarily to evapotranspiration (Brinson, 1993). However, outlets have been artificially created by some landowners to drain wetlands and increase area for cultivated land. Outlets are also present on some of the larger water bodies that are part of the stream network. These larger water bodies can be classified as shallow water wetlands because they are in a stage between marsh and lake.

The climate in nearby Yorkton (70 km west of SCRB) is characterized by average July and January temperatures of 18°C and -19°C, respectively. Between 1971 and 2000, annual average precipitation was ~450 mm with 75% falling as rain. Streamflow is generated primarily by spring snowmelt, with peak streamflow occurring in late April and subsiding to substantially lower or intermittent flows throughout the summer (Figure 2.2).

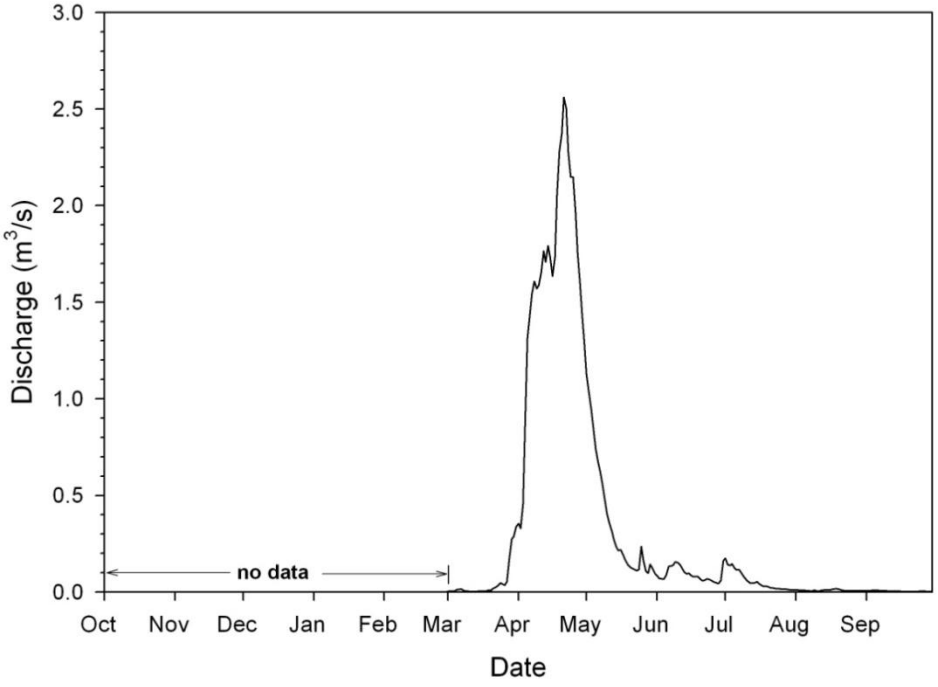

Figure 2.2. Mean daily discharge (1975-2006) for Smith Creek near Marchwell (05ME007). Average discharge per year = 0.27 m^3/s, standard deviation = ±1.22 m^3/s.

2.1.2 Denis National Wildlife Area

The second study site was the St. Denis National Wildlife Area (SDNWA), which is located 40 km east of Saskatoon (106° 06' W and 52° 02' N; Figure 2.3). This site represents a different type of PPR topography than SCRB as it has fewer impacts from agriculture and has greater topographic relief. SDNWA has ~100 wetlands with extensive long term water level records and was one of the sites used by Hayashi and van der Kamp (2000). This site was ideal for meeting the objectives of this thesis because Hayashi and van der Kamp provided the topographic survey data used in their research.

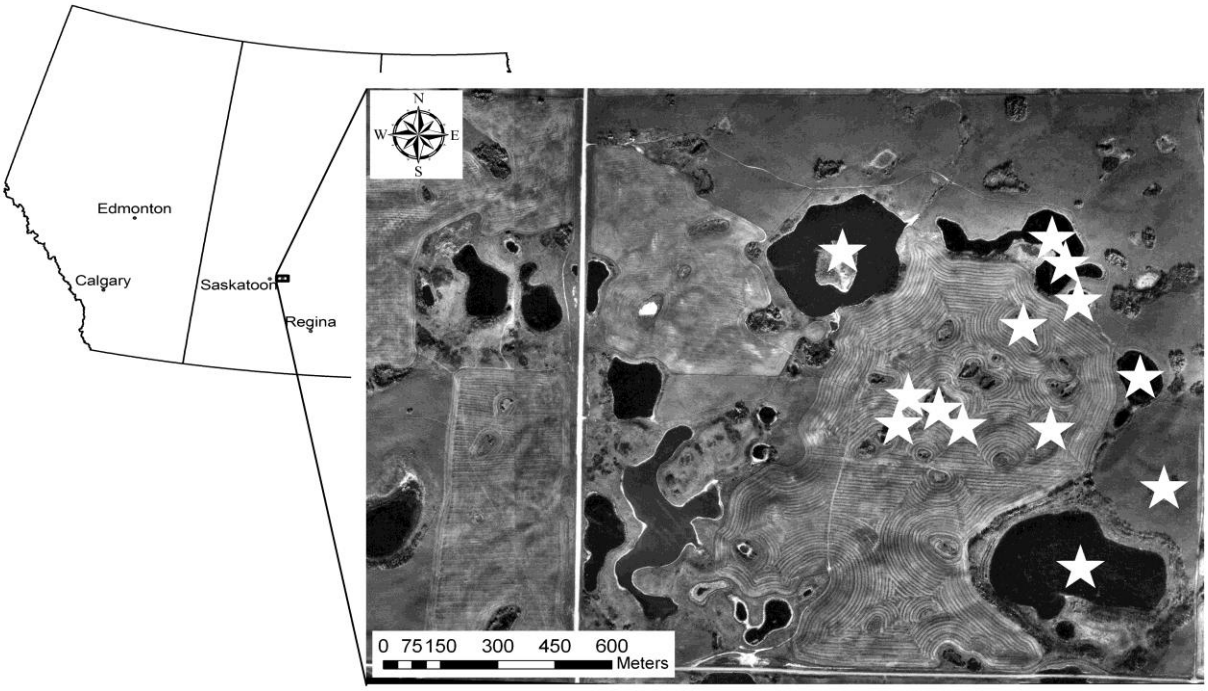

Figure 2.3. Aerial photo (1997) of the St. Denis National Wildlife Area (SDNWA) depicting wetlands with survey data (stars).

SDNWA is ~4 km^2 and is part of a larger 24 km^2 watershed. The watershed is internally drained except in extremely wet years (van der Kamp and Hayashi 2009). The topography is described as rolling knob and kettle moraine, with slopes of 10-15% (Miller et al. 1985). The majority of wetlands in SDNWA are located in small depressions, with the exception of a few very large, deep wetlands. The region is typical of the prairie landscape with glacial deposits consisting mostly of clay with low permeability (Hayashi et al. 1998). The land use of SDNWA was dominated by cultivation until the mid-1980's when approximately one-third of it was converted to natural grassland (van der Kamp et al. 1999). The average temperature range at nearby Saskatoon is the same as Yorkton; however, annual average precipitation is 350 mm with 76% occurring as rain.

2.2. Measurement of Actual Wetland Volume and Area

Within SCRB, 14 wetlands were selected for a detailed topographic survey. Topographic data were available for 13 wetlands in SDNWA (data provided by M. Hayashi, University of Calgary and G. van der Kamp, Environment Canada). In SCRB, an electronic total station was used to collect coordinates with ~1 m spacing in the wetland and upland. An attempt was made to collect enough points in the upland so the point at which water spills from the wetland was included. However, for some wetlands, this was not possible because vegetation restricted the total station line of sight. On average, 150 elevation points were gathered for each wetland. Eight of the SDNWA wetlands were surveyed with a total station (Hayashi and van der Kamp 2000), while topographic data for the others (S1, S90, S97, S124, and S125) were collected with a hand-held GPS and a sounding rod to measure water depth. Survey data were used to generate a three-dimensional, 1-m resolution digital elevation model (DEM) for each wetland in Surfer, version 8 (Golden Software, Golden, CO, USA). Data were interpolated using ordinary kriging (Cressie 1990) with a linear variogram and no drift to create a 1-m resolution DEM (Zimmerman et al. 1999, Hayashi and van der Kamp 2000). The actual volume and surface area were calculated for each topographic survey-derived DEM using the grid volume function in Surfer. These measurements were calculated at 0.05 m depth increments starting at 0.1 m above the lowest point in the wetland (h_{min}) to the depth where the depression capacity is exceeded (h_{max})(Figure 2.4a). For this research, volumes were estimated using the full and simplified Hayashi-van der Kamp *V-A-h* method (section 2.3) and the LiDAR *V-A-h* method (section 2.5). These estimated volumes and areas were compared to the actual ones using the root-mean-squared (RMS) error (Hayashi and van der Kamp 2000)

$$V_{err} = \sqrt{\frac{1}{n}\sum_{i=1}^{n}(DEM - EST)^2} \qquad (2.1)$$

where n is the number of data points. DEM represents either the actual volume or area calculated from the topographic survey-derived DEM, while EST represents either the volume or area estimated by the *V-A-h* method. The magnitude of error, in percent, was calculated by dividing V_{err} and A_{err} by the actual volume and area at a certain evaluation depth (referred to as V_{eval} and A_{eval}). Hayashi and van der Kamp (2000) recognized that the magnitude of error increases as the evaluation depth is set closer to h_{min}. As a result, V_{eval} and A_{eval} should not be set to h_{max} or a depth near h_{min} because the magnitude of error would not adequately represent the accuracy of the volume or area estimation. The depth interval closest to 80% of h_{max} was used for V_{eval} and A_{eval} because this depth is usually reached each spring when the maximum volume would be estimated. These values were consistent with the V_{eval} and A_{eval} depths of between ~80% and 100% of h_{max} that Hayashi and van der Kamp (2000) used.

2.3. Assessing Robustness of the Hayashi-van der Kamp Method Across the PPR

2.3.1. Quantifying Wetland Surface Area Shape

Hayashi and van der Kamp (2000) developed the full *V-A-h* method on natural, relatively regularly shaped wetlands at SDNWA. To assess the robustness of their full and simplified method, wetlands were selected that would represent the range of morphologies observed in the PPR. To characterize the surface area shape, the perimeter of each wetland pond was delineated from aerial photography. Imagery from 2000 was used for SCRB. Multiple years (1968, 1970, 1980, 1985, and 1997) were used for SDNWA to capture the pond shape when elevation data

were collected. In addition to the surveyed wetlands, 100 wetlands in SCRB were randomly selected for digitizing so the range of pothole surface area shape in the watershed was fully represented. A power regression line was fitted to these data to obtain a frequency curve which characterizes the distribution of wetland shapes in SCRB. Inconsistent perimeter measurements were avoided by using a constant step length (i.e., distance) of 2 m between nodes in the GIS. This prevented the scaling effect of fractal objects, as described by Mandelbrot (1967), where perimeter measurements increase when a smaller step length is used. Perimeter and area were calculated by using the geometry function in ArcGIS, version 9.2 (ESRI, Redlands, CA, USA). Measurements for each wetland were used to calculate the shape index, SI (McGarigal and Marks 1995), as follows:

$$SI = \frac{P}{2\sqrt{\pi A}} \qquad (2.2)$$

where SI is defined as the ratio of the wetland perimeter (P) to the circumference of a circle with the same area (A) as the wetland of interest (Forman and Godron 1986; Appendix A). If the wetland of interest were a perfect circle then the SI value would equal one. While natural wetlands may be very similar to a circle (e.g., SI = 1.01), they will never be a perfect circle and thus will have an SI > 1 (Appendix A). Therefore, wetlands that are similar in shape to a circle have an SI value close to one and are considered regularly shaped. While wetlands that are more irregular will have a higher SI value. Unlike previous indices that describe the inverse, non-linear ratio of P to A (Millar 1971, Brooks and Hayashi 2002), the square root of area is used for the SI to make it dimensionless and ensure that values are comparable for small and large wetlands.

2.3.2. Estimating Area and Volume with the Hayashi-van der Kamp Methods

Hayashi and van der Kamp (2000) presented two simple equations for estimating wetland pond area and volume

$$A = s\left(\frac{h}{h_o}\right)^{2/p} \quad (2.3)$$

$$V = \frac{s}{(1+2/p)} \times \frac{h^{1+(2/p)}}{{h_0}^{2/p}} \quad (2.4)$$

where *s* represents the size of the wetland, *p* represents the depression profile, *h* is the depth of water (m) above the lowest point of the wetland (h_{min}), and h_o is the unit depth (h_o = 1 m). The *s* coefficient is further defined as the actual area of the wetland when water depth is equal to the unit depth ($h = h_0$). For example, if the unit of depth is meters then the *s* coefficient represents the area (m^2) of the pond when *h* = 1 m. The *p* coefficient is further defined as a power coefficient that represents the wetland as a symmetrical, concave depression. A small *p* value (e.g., *p* = 2) "corresponds to a paraboloid basin that has smooth slopes extending from the center to the edge, and a large value corresponds to a basin that has a flat bottom" (Hayashi and van der Kamp 2000).

The *A*-*h* relationship for each wetland needed to be characterized to determine the *s* and *p* coefficients required for estimating volume and area though the full Hayashi-van der Kamp *V*-*A*-*h* method. Therefore, the surface area and depth calculated from the survey DEM (section 2.2) were plotted on a log-log graph. A power regression line was fitted to these data to obtain the *s*

and *p* coefficients required for the full *V-A-h* method. Since a power regression line can be generalized as $y = ax^b$, the *s* coefficient is equal to "a" and the *p* coefficient is equal to 2 divided by "b". The *s* and *p* coefficients for each wetland were used in Eq. 2.3 and 2.4 to estimate area and volume at 0.05 m depth increments from $h = 0.1$ m to h_{max}.

Hayashi and van der Kamp (2000) suggested a simplified *V-A-h* method that could be used to derive the *s* and *p* coefficients when detailed survey data are not available. The simplified *V-A-h* method only requires concurrent measurements of surface area and depth at two points in time, provided that Δh and $\Delta A > 0$. Equations 2.3 was modified so that the coefficients could be directly calculated using

$$p = 2\left(\frac{\log(h_1/h_2)}{\log(A_1/A_2)}\right) \tag{2.5}$$

$$s = A_1\left(\frac{h_1}{h_o}\right)^{-2/p} \tag{2.6}$$

where A_1 and A_2 are the surface area measurements at the depths, h_1 and h_2 (Figure 2.4). Since Hayashi and van der Kamp did not specify when area and depth should be measured, two scenarios were examined for collecting the measurements required for the simplified *V-A-h* method. The first scenario mimicked a hydrologically dry year when a limited range of area and depth measurements would be available. Scenario 1 is referred to as the 'simplified *V-A-h* method for drought conditions'. The second scenario involved a wider range of area and depth values that spanned the average wetland storage capacity. Scenario 2 is referred to as the 'simplified *V-A-h* method for average or wet conditions'. When applying either of the simplified

methods the area and depth measurements used were from the topographic survey-derived DEM (section 2.2). This allowed for a range of scenarios to be tested without having to collect additional measurements.

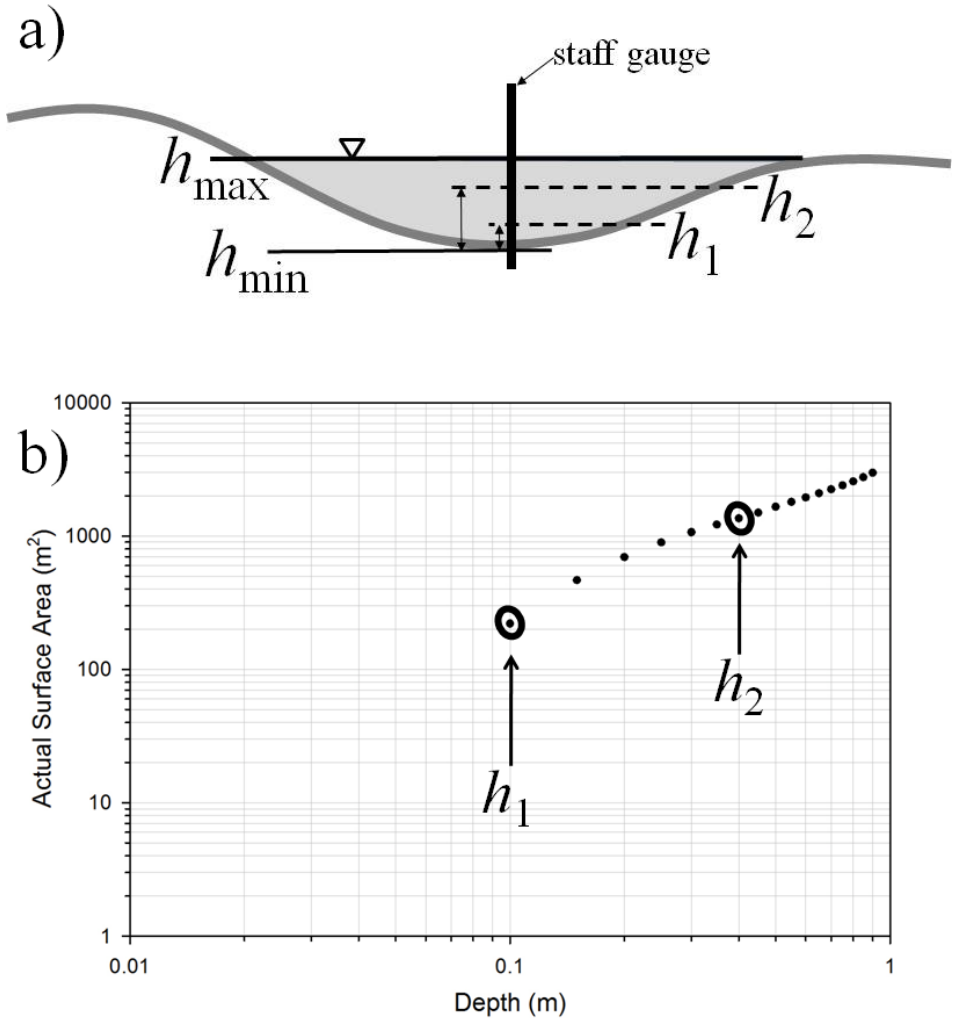

Figure 2.4. a) Profile of a hypothetical wetland illustrating: h_{min} – the lowest point in the wetland; h_{max} – the maximum depth of water before the depression capacity is exceeded; h_1 and h_2 – arbitrary depths at which area are measured for the simplified *V-A-h* method. Exact values of h_1 and h_2 are user defined, provided that $h_1 < h_2$. b) Characterizing the *A-h* relationship through a log-log graph where h_1 and h_2 correspond to surface area measurements, A_1 and A_2.

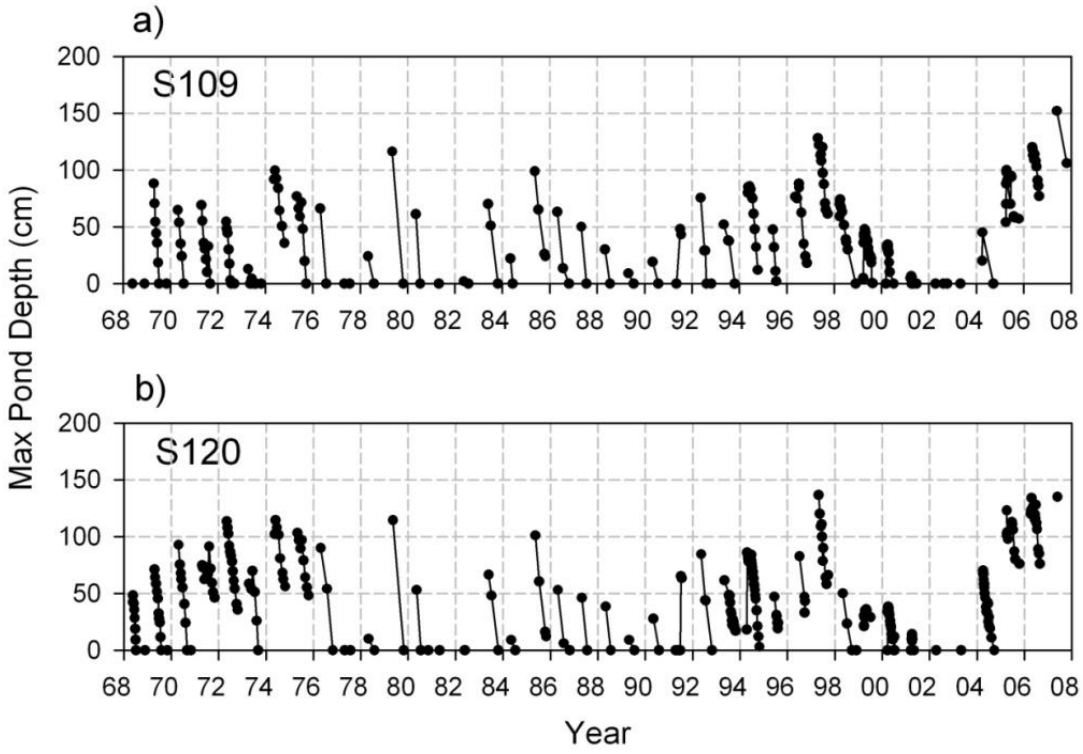

Figure 2.5. Water depths from 1968 to 2007 for a) pond S109 and b) pond S120 in SDNWA (data courtesy of G. van der Kamp).

The 1968-2007 water level records for SDNWA were analyzed to identify the depths for which surface area should be measured for both simplified *V-A-h* scenarios. The average maximum water depth for wetlands in Hayashi and van der Kamp's (2000) study (S92, S109, S120, S125s, and S104) is ~0.58 m, which is approximately 50% of h_{max} for these wetlands. Furthermore, there were many years where the average water depth was below 0.2 m, i.e., ~25% of h_{max}. For example, wetlands S109 and S120 illustrate these water level fluctuations because they did not exceed a 0.2 m maximum depth more than ~25% of the time (Figure 2.5). From this analysis, and from water levels published for other PPR wetlands (Winter and Rosenberry 1998, Fang and Pomeroy 2008), it is apparent that many periods of drought have impacted wetland water levels across the prairies. Thus, there are many years when low water levels are a barrier to

collecting surface area and depth measurements. Therefore, for scenario 1 the *s* and *p* coefficients were derived from area and depth measurements that would reflect drought-like conditions. When applying the simplified *V-A-h* method for drought conditions, the surface area measurements used were at h = 0.1 and 25% of h_{max}. For some shallow wetlands 25% of h_{max} was not greater than 0.1 m, therefore a depth of 0.15 m was used. For each wetland, the area and depth measurements were inserted into Eq. 2.5 and 2.6 to generate the *s* and *p* coefficients. Although *s* and *p* values were derived from drought-like conditions, these values were used to estimate area (Eq. 2.3) and volume (Eq. 2.4) at 0.05 m depth increments from h = 0.1 m to the maximum depth of each wetland (h_{max}). Eq. 2.1 was used to calculate the goodness of fit between the actual and estimated area and volume.

When applying the simplified *V-A-h* method for average or wet conditions (scenario 2), the area and depth measurements spanned the wetland storage capacity to calculate *s* and *p*. Given the seasonal fluctuation of wetland water levels (Figure 2.5) due to snowmelt and evapotranspiration, measurements that span the storage capacity of a wetland would include a depth measurement near h_{max} in spring and a minimum measurement when water levels have declined. For semi-permanent wetlands, the minimum water depth is likely to occur in late summer or fall, prior to the wetland freezing. With temporary or seasonal wetlands, the minimum water depth is likely to occur in mid-summer before the pond completely dries out. The surface area measurements used for the simplified *V-A-h* method for average or wet conditions were those when h = 0.1 m and h = ~50% of h_{max}. The maximum value was chosen because the water level analysis identified an average depth of ~0.58 m, which represents approximately 50% of h_{max} over the 39 year record at SDNWA. These values of area and depth were used to derive the unique *s* and *p* coefficients (Eq. 2.5 and 2.6) for each wetland and were

used to estimate area (Eq. 2.3) and volume (Eq. 2.4) at 0.05 m depth increments from h = 0.1 m to h_{max}. Eq. 2.1 was used to test the goodness of fit.

2.3.3. Sensitivity Analysis of the Simplified *V-A-h* method

Since both simplified *V-A-h* scenarios rely on surface area and depth measurements to derive the *s* and *p* coefficients, an analysis was conducted to assess the sensitivity of volume error to the potential variability when measuring area and depth. For the area analysis, error in delineated the wetted perimeter of a pond was simulated to assess the effect on volume estimation. Pond S120 from SDNWA was selected for this analysis because the ponds' wetted perimeter is difficult to define from air photos (Figure 2.6) and thus, would be subject to error depending on the method used. Pond S120 represents a typical PPR wetland with a h_{max} of 1.1 m and an A_{max} of 3150 m^2. Area at two depths which are normally reached each year (A_1 at h = 0.1 m, A_2 at h = 0.45 m) were used for the simplified *V-A-h* method. The actual wetted perimeters at these depths were selected from the topographic survey-derived DEM and exported to ArcGIS where area was calculated using the geometry function. The buffer tool was used in ArcGIS to create a new perimeter boundary at 0.5 m increments from -3.0 m to +5.0 m from the actual perimeter (Figure 2.6). Three types of perimeter analyses were conducted: 1) the perimeters for A_1 and A_2 were varied the same distance, ranging from -3 m to +5 m, 2) the actual perimeter for A_1 was held constant while A_2 was varied from -3 m to +5 m, and 3) the perimeter for A_1 was varied from -3 m to +5 m while the actual perimeter at A_2 was held constant. The *s* and *p* coefficients were derived for each perimeter analysis using Eq. 2.5 and 2.6. These coefficients were used to estimate volume at 0.05 m depth increments from h = 0.1 m to h_{max} using Eq. 2.4. The root-mean-square error was calculated (Eq. 2.1) to test the goodness of fit.

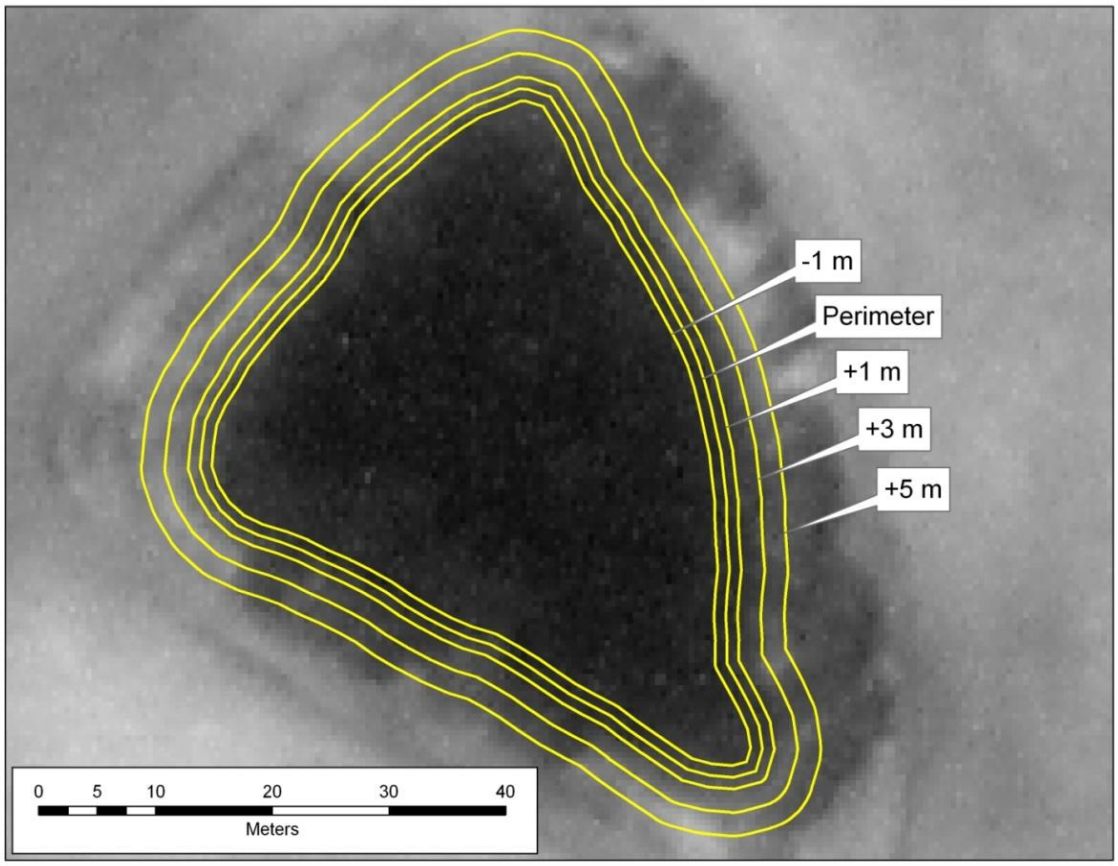

Figure 2.6. Air photo (1980) of pond S120 illustrating perimeter boundaries generated to assess the effect of wetted perimeter delineation error on area calculation (limited perimeters shown). In the analysis, perimeter for h = 0.1 m and h = 0.45 m was varied from -3 m to +5 m of the actual perimeter in 0.5 m increments.

When analyzing the depth measurements, the depth at which A_2 is measured was varied to assess the effect on volume estimation for the simplified *V-A-h* method. A_2 was investigated because this area could potentially be measured at any depth from h_1 up to h_{max} (Figure 2.4). Therefore, three wetlands (D2, W7, and W2; Appendix C) with varying morphologies had A_2 varied from h = 0.15 m to h_{max} by 0.05 m depth increments. Each combination of A_1 and A_2 were used to calculate the *s* and *p* coefficients (Eq. 2.5 and 2.6). These coefficients were used to estimate volume (Eq. 2.4) at 0.05 m depth increments from h = 0.1 m to h_{max}. Eq. 2.1 was used to test the goodness of fit.

2.4. Acquisition of LiDAR Data

LiDAR data were collected in October 2008 (SCRB) and August 2005 (SDNWA). Data were collected and processed by LiDAR Services International Incorporated for SCRB and Canadian Consortium for LiDAR Environmental Applications Research (C-CLEAR) for SDNWA. A Riegl LMS-Q560 sensor was used for SCRB data collection and an ALTM3100 sensor was used for SDNWA (Töyrä et al. 2006). Flight parameters are presented in Table 2.1.

Table 2.1. Sensor settings for LiDAR data acquisition

Parameter	SCRB	SDNWA
Aircraft altitude (m.a.g.l)	600	1,500
Flying Speed (km/h)	225	200
Laser Frequency (kHz)	150	50
Scan Angle (°)	± 30	± 14
Strip Overlap (%)	30	50

Differential global positioning systems located on a local benchmark and attached to the aircraft were used in conjunction with an inertial navigation unit to record aircraft location at all times. Laser pulses were actively transmitted toward the ground surface in the near-infrared wavelength. Post-processing classified the laser return pulses as bare ground, vegetation or man-made objects based on the return time of the pulse. Pulses that took the longest time to return to the sensor were classified as the actual ground surface and were used to create a 1-meter resolution, bare-earth DEM. The average laser point spacing was 0.66 m (SCRB) and 0.5 m (SDNWA; Töyrä et al. 2006). Ground control points (GCP) were collected independently of the LiDAR acquisition to verify the data accuracy. In SCRB, the average difference between the ground surface and the LiDAR DEM was -0.01 m, the maximum absolute difference was 0.29 m, and the RMS error was 0.05 m. In SDNWA, the average difference was 0.03 m, the maximum absolute difference was 1.45 m, and the RMS error was 0.14 m (Töyrä et al. 2006).

The discrepancy between maximum absolute differences for each site was due to the type of topography in which GCPs were located. While data verification for SDNWA incorporated wetland vegetation at selected locations, the SCRB verification did not. However, Ducks Unlimited Canada performed additional data verification in SCRB and found that wetland elevation values had a maximum absolute difference of 1.32 m (L. Boychuck, unpublished data). Thus, the vertical accuracy for each site is comparable at approximately <0.2 m.

2.5. Theory for Applying the Simplified *V-A-h* Method to a LiDAR DEM

The simplified *V-A-h* method provides an easy way to derive the *s* and *p* coefficients. Hayashi and van der Kamp (2000) suggested that a constant *p* value of 2 could be used for small natural wetlands when time and resources are limited. If a constant *p* value is assumed then it would only be necessary to calculate the *s* coefficient (Eq. 2.6). The required data for calculating the *s* coefficient is the surface area (A_1) at h_1 (Figure 2.7). While LiDAR pulses can partially penetrate the water surface, they cannot provide information on the depth of water (h_1) because the near-infrared pulse (i.e., 0.7 – 1.4 µm) is easily scattered. While shorter wavelengths (e.g., 0.5 µm) can penetrate the water surface, prairie wetlands often do not have the ideal conditions, such as low turbidity, minimal vegetation, or a reflective substrate (Töyrä and Pietroniro 2005, Legleiter et al. 2009), that would allow depth information to be acquired. Even though the depth of water cannot be measured, it is still possible measure A_1, A_2, and Δh through GIS analysis. By assuming a constant *p* value and rearranging Eq. 2.3, it is possible to use the measurements of A_1, A_2, and Δh to calculate the depth of water at the time of LiDAR data acquisition.

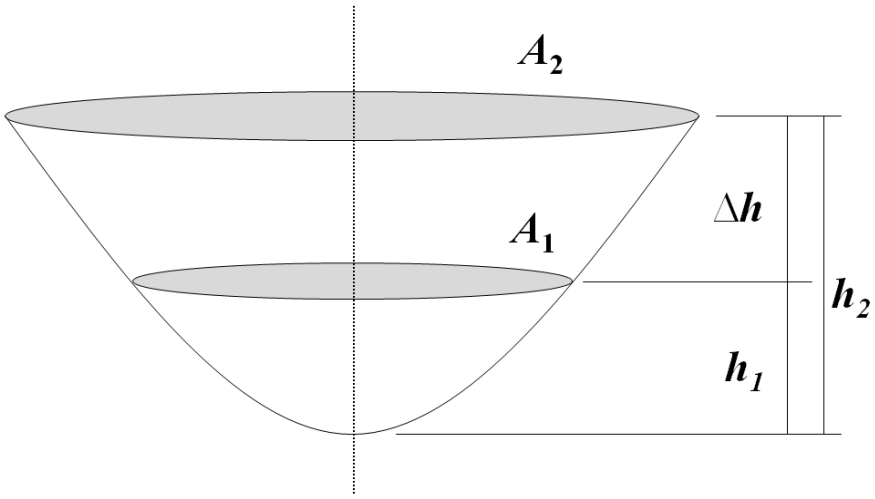

Figure 2.7. Theoretical wetland illustrating area and depth measurements required for applying the simplified *V-A-h* method to a LiDAR DEM. See text for definition of terms.

The Hayashi-van der Kamp equation for estimating area (Eq. 2.3) can be written to solve for the surface area at a certain depth through

$$A_1 = s\left(\frac{h_1}{h_o}\right)^{2/p} \tag{2.7}$$

where h_1 is the depth of water when A_1 is measured (Figure 2.7). Similarly, h_2 can be inserted into the above equation to calculate A_2. The equation for A_2 can be divided by A_1 to give

$$\frac{A_2}{A_1} = \left(\frac{h_2}{h_1}\right)^{2/p} \tag{2.8}$$

This equation can be rewritten to solve for h_2 (Appendix B). However, since only Δh is known the equation for h_2 must be inserted into $\Delta h = h_2 - h_1$, and rewritten to solve for h_1 through

$$h_1 = \frac{\Delta h}{(A_2/A_1)^{p/2} - 1} \qquad (2.9)$$

With h_1 and A_1 known, the *s* coefficient can be calculated (Eq. 2.6) and used along with the constant *p* coefficient to estimate volume (Eq. 2.4).

2.6. Comparing to *V-A* Equations

Wetland volume was estimated with two sets of *V-A* equations to make comparisons with the LiDAR *V-A-h* method. One equation that was developed for the Upper Assiniboine River Basin study (Manitoba Conservation, 2000) by Wiens (2001) is suitable for estimating volume for wetlands smaller than 70 hectares through

$$V = 2.85A^{1.22} \qquad (2.10)$$

where *A* is in hectares and *V* is in cubic decameters. This equation has since been used to estimate wetland storage across Saskatchewan (Wiens 2001, SWA 2008). The second group of equations were developed for the three major physiographic regions in the PPR by the United States Geological Survey (USGS, Gleason et al. 2007). These regions are the glaciated plains (Eq. 2.11), Prairie Coteau (Eq. 2.12), and Missouri Coteau (Eq. 2.13; Gleason et al. 2007)

$$V = 0.25A^{1.4742} \quad (2.11)$$

$$V = 0.458A^{1.5611} \quad (2.12)$$

$$V = 0.398A^{1.542} \quad (2.13)$$

where A is in hectares and V is in hectare-meters. Volume was calculated with each equation to evaluate whether the appropriate physiographic equation provides the most accurate estimate of volume. The *V-A* equations were applied to surface area measurements derived from the topographic survey (Section 2.1) and were used to estimate volume at h_{max}.

CHAPTER 3 – ROBUSTNESS OF THE HAYASHI-VAN DER KAMP METHOD

3.1. Results

The 100 randomly selected wetlands in Smith Creek ranged in surface area shape from 1.0 to 2.2 (Figure 3.1, power regression line), with 95% of these wetlands having an SI < 1.6. The 14 wetlands in SCRB and the 13 in SDNWA selected for detailed study covered most of this range. The full *V-A-h* method estimated volume and area very well for all wetland shapes (Table 3.1); RMS errors were ≤5% for volume and area (Figure 3.2). There was no relationship between volume percent error and SI ($r^2 = 0.005$, P = 0.725) and a weak relationship between area percent error and SI ($r^2 = 0.198$, P = 0.021).

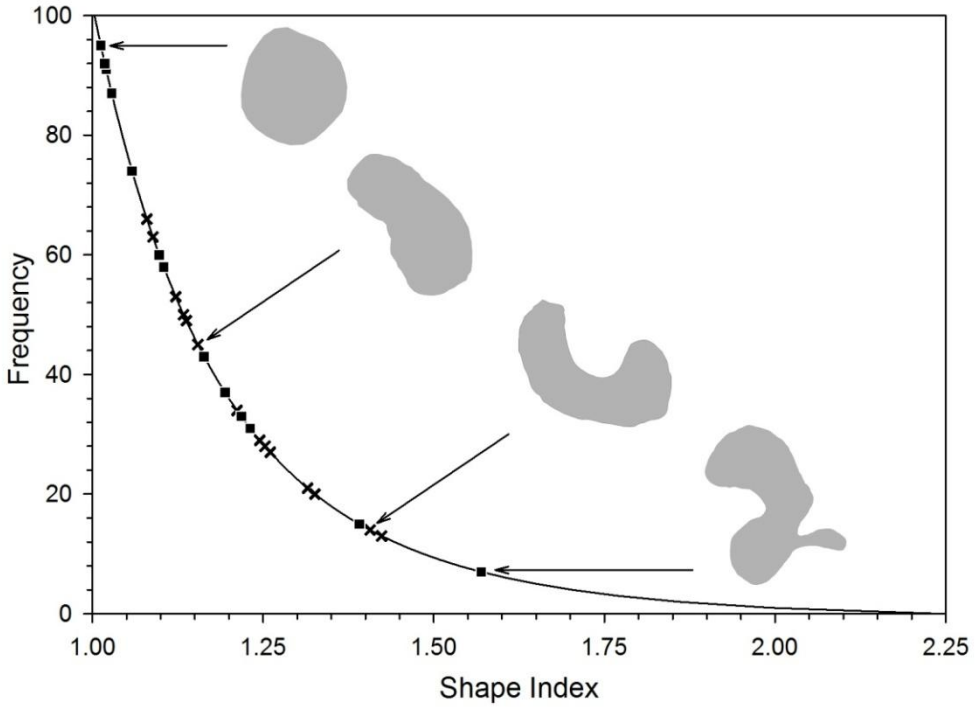

Figure 3.1. The power regression line shows the frequency distribution of 100 wetland surface shapes in the Smith Creek Research Basin. Shown are the wetlands studied in Smith Creek watershed (**x**) and St. Denis NWA (■). Shaded illustrations are surface shapes for wetlands (left to right) D2, W10, W2, S125. See Eq. 2.2 for computation of the shape index.

Table 3.1. Shape index values for each wetland calculated from area and perimeters measured from air photos for certain years. h_{max}, A_{eval}, V_{eval}, s and p derived from the full *V-A-h* method and the associated errors for wetlands in SCRB and SDNWA. Wetlands are organized according to increasing SI for each site.

Wetland ID	SI	A (m^2)	P (m)	Air Photo Year	h_{max} (m)	A_{eval} & V_{eval} (m)	s (m^2)	p	A_{err} (m^2)	A_{err}/A_{eval} (%)	V_{err} (m^3)	V_{err}/V_{eval} (%)
Smith Creek												
LR4	1.079	2471	190	2000	0.85	0.70	4686	1.54	35.45	1.23	5.22	0.58
W8	1.089	908	116	2000	0.45	0.35	3172	1.49	20.43	2.72	2.27	1.94
W1	1.124	1355	147	2000	0.65	0.50	2829	1.74	24.47	1.97	2.78	0.94
W11	1.131	1957	177	2000	0.45	0.35	6481	1.77	31.08	1.60	3.39	1.05
B1	1.138	1987	180	2000	0.90	0.70	3218	2.07	48.52	2.17	9.79	1.22
W10	1.155	1667	167	2000	0.90	0.70	2035	1.47	31.42	2.53	5.80	1.56
W4	1.217	1915	189	2000	0.50	0.40	5004	1.62	49.08	3.20	3.62	1.27
W3	1.250	1527	173	2000	0.50	0.40	11366	0.84	59.84	4.98	8.09	5.00
W7	1.253	1475	171	2000	0.50	0.40	3792	1.69	35.27	2.79	4.46	1.92
LR3	1.262	8963	424	2000	1.10	0.90	12571	1.88	435.93	4.00	82.87	1.69
LR7	1.318	9309	451	2000	0.75	0.60	16456	2.06	329.70	3.20	58.87	1.93
LR2	1.326	1684	193	2000	0.50	0.40	6245	1.85	25.68	1.12	1.61	0.36
W2	1.409	3269	286	2000	0.60	0.50	8876	1.82	186.59	4.58	33.02	3.42
W9	1.420	4570	340	2000	0.70	0.55	10012	2.10	94.73	1.70	21.13	1.34
St. Denis												
D2	1.012	227	54	1970	0.45	0.35	951	1.62	5.38	2.11	1.55	3.74
S104	1.018	961	112	1985	0.70	0.55	1763	1.95	16.69	1.77	2.71	1.04
D3	1.020	453	77	1970	0.70	0.55	1121	1.68	13.65	2.54	2.57	1.84
S124	1.028	1861	157	1970	0.60	0.50	3205	1.89	12.63	0.82	3.91	1.05
S97	1.059	7924	334	1997	0.70	0.55	12926	3.33	114.02	1.28	56.87	1.87
D1	1.099	377	76	1968	0.30	0.25	3695	1.39	10.55	2.15	1.68	3.18
S109	1.107	2457	194	1985	1.20	0.95	3183	1.63	103.60	3.60	19.42	1.53
S120	1.162	1599	165	1980	1.10	0.90	2798	2.69	57.80	2.27	10.54	0.80
S1	1.195	74054	1152	1997	2.65	2.10	21570	1.67	1126.48	2.11	314.23	0.62
S125s	1.218	3711	263	1970	1.35	1.10	4209	1.79	101.04	2.14	25.20	1.04
S90	1.232	96603	1358	1997	3.40	2.70	79084	3.40	1479.65	1.05	675.26	0.28
S92	1.398	888	148	1980	1.20	0.95	2438	1.84	89.99	4.09	14.53	1.39
S125	1.572	22898	843	1980	1.80	1.45	10855	1.64	543.76	3.22	231.40	2.09

The simplified *V-A-h* method was examined to test its robustness for two scenarios: 1) a hydrologically dry year, and 2) an average or wet year. For the drought scenario, thirteen of the 27 wetlands (48%) had volume errors greater than 10% (Figure 3.3a), which is the error that Hayashi and van der Kamp (2000) advocate as being acceptable. In some instances (e.g., B1, W2, and W7), volume errors exceeded 40% and approached 290%. Nineteen of the 27 wetlands (70%) exceeded area errors of 10% (Figure 3.3a). Wetlands B1, W2, and W7 had area errors greater than 70% and approached ~550%. For the average or wet scenario, volume errors were <10.5% for all wetlands but W2, and area errors of <10% for nine of the 27 wetlands (33%) (Figure 3.3b).

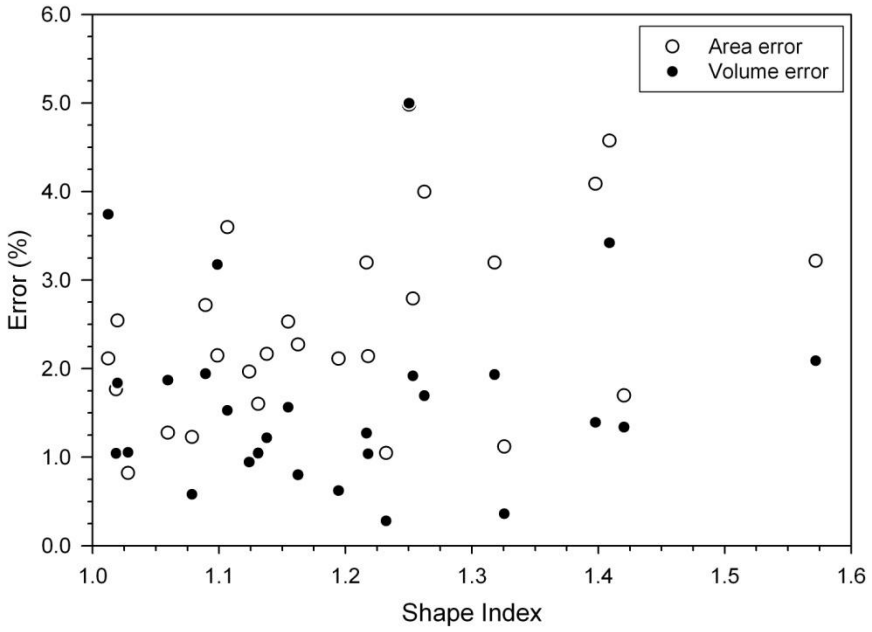

Figure 3.2. Illustration of the relationship between wetland surface area shape (shape index) and errors from the full Hayashi-van der Kamp *V-A-h* method. Wetlands with a more irregular surface area shape have a higher shape index value. No relationship was found for volume error vs. shape index ($r^2 = 0.005$, $P = 0.725$), while a statistically significant, linear relationship was found for area error vs. shape index ($r^2 = 0.198$, $P = 0.021$).

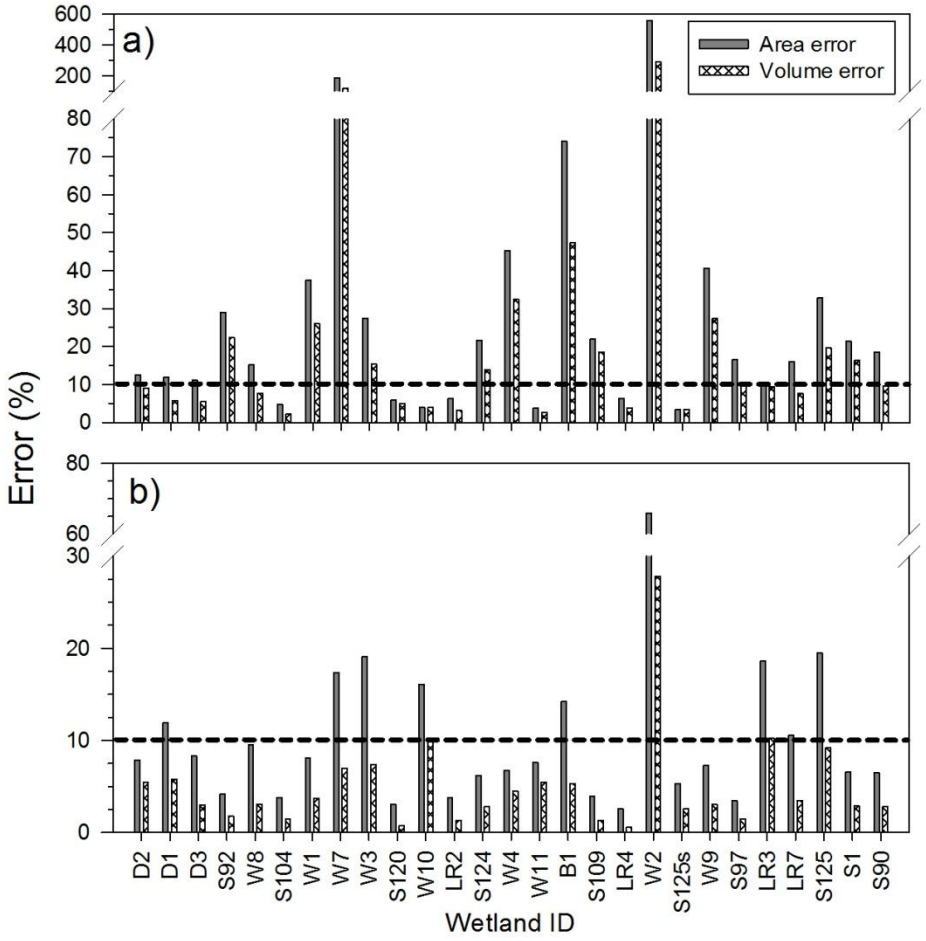

Figure 3.3. Error from using a) scenario 1: the simplified *V-A-h* method for drought conditions, and b) scenario 2: the simplified *V-A-h* method for average or wet conditions. Wetlands are organized from left to right according to increasing A_{max}. Dash line represents the 10% error limit. Upper error limit (%) is different for scenario 1 (a) and scenario 2 (b).

To illustrate how different *s* and *p* coefficients can be derived from scenarios 1 and 2 the survey-derived graph of area against depth for W2 is presented (Figure 3.4a). From *h* = 0.1 to 0.2 m the rate of surface area increase is relatively rapid because of the depression morphology (Figure 3.4b). However, when the wetland is filled above the 0.2 m depth, the rate of surface area increase slows. Thus, this wetland would have very different *s* and *p* coefficients depending of the *A-h* combination used.

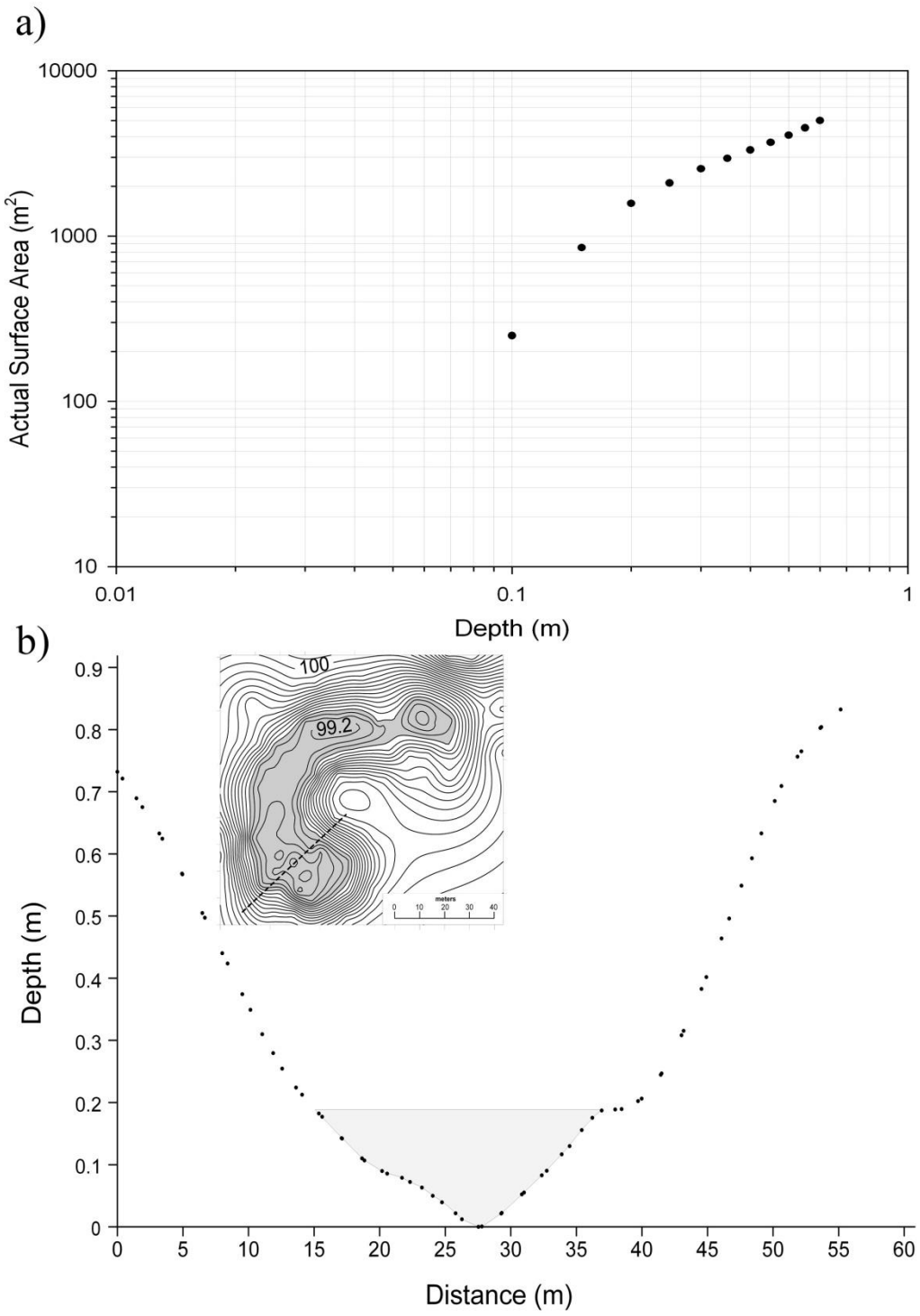

Figure 3.4. *A-h* relationship determined from the topographic survey-derived DEM for wetland W2 at SCRB. Full *V-A-h* method provides an $s = 8876$ and $p = 1.82$ in this example (Table 3.1). b) Cross-section through the deepest point of wetland W2 to illustrate basin morphology. Inset: plan view of wetland W2 with 0.05 m elevation contours and water level at the time of surveying shown in gray shading.

The sensitivity analysis of wetted perimeter delineation showed a linear increase in volume error with distance from the actual wetted perimeter (Figure 3.5). Volume error increased most rapidly when the wetted perimeter for A_1 (at h = 0.1 m) was held constant and A_2 (at h = 0.45 m) was varied. In this situation, errors exceeded 10% when the wetted perimeter was located more than +1.5 m or less than -2.0 m away from the actual perimeter.

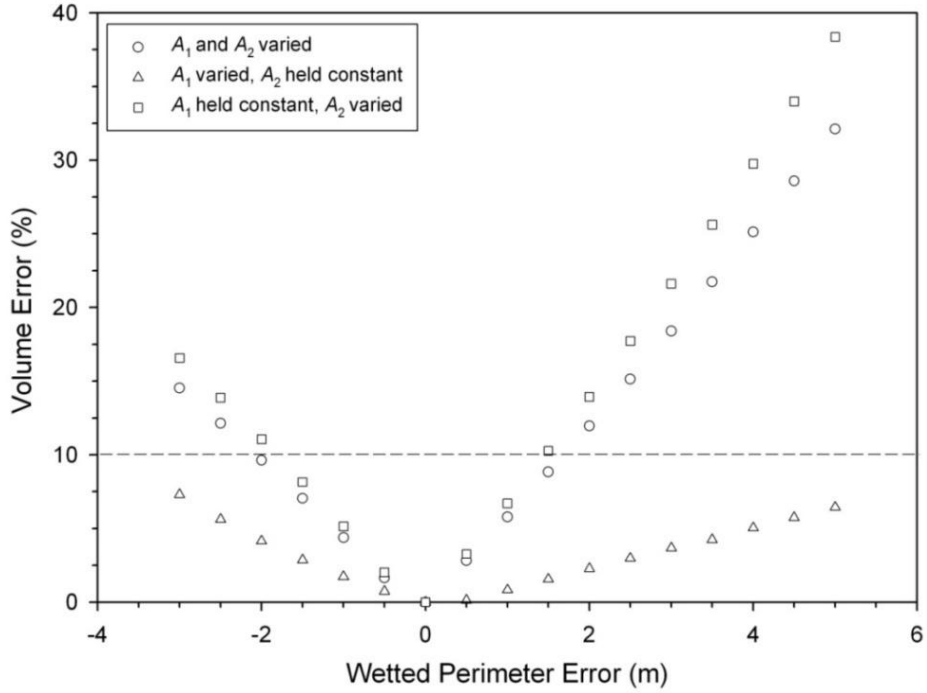

Figure 3.5. Volume error for pond S120 at SDNWA when the wetted perimeter is delineated incorrectly. A_1 at h = 0.1 m and A_2 at h = 0.45 m were used when implementing the simplified *V-A-h* method. Perimeters were varied from -3.0 m to +5.0 m of the actual perimeter.

The depth analysis showed that volume errors were highest when A_2 was measured at a shallow depth (i.e., smaller percent of h_{max}), while the minimum volume error occurred when A_2 was between ~60-80% of h_{max} (Figure 3.6). The range in volume error was smallest for the

wetland with the most regular morphology (D2, range of 5%), while the most irregular wetland had the largest range (W2, range of 280%) in volume error (Figure 3.6).

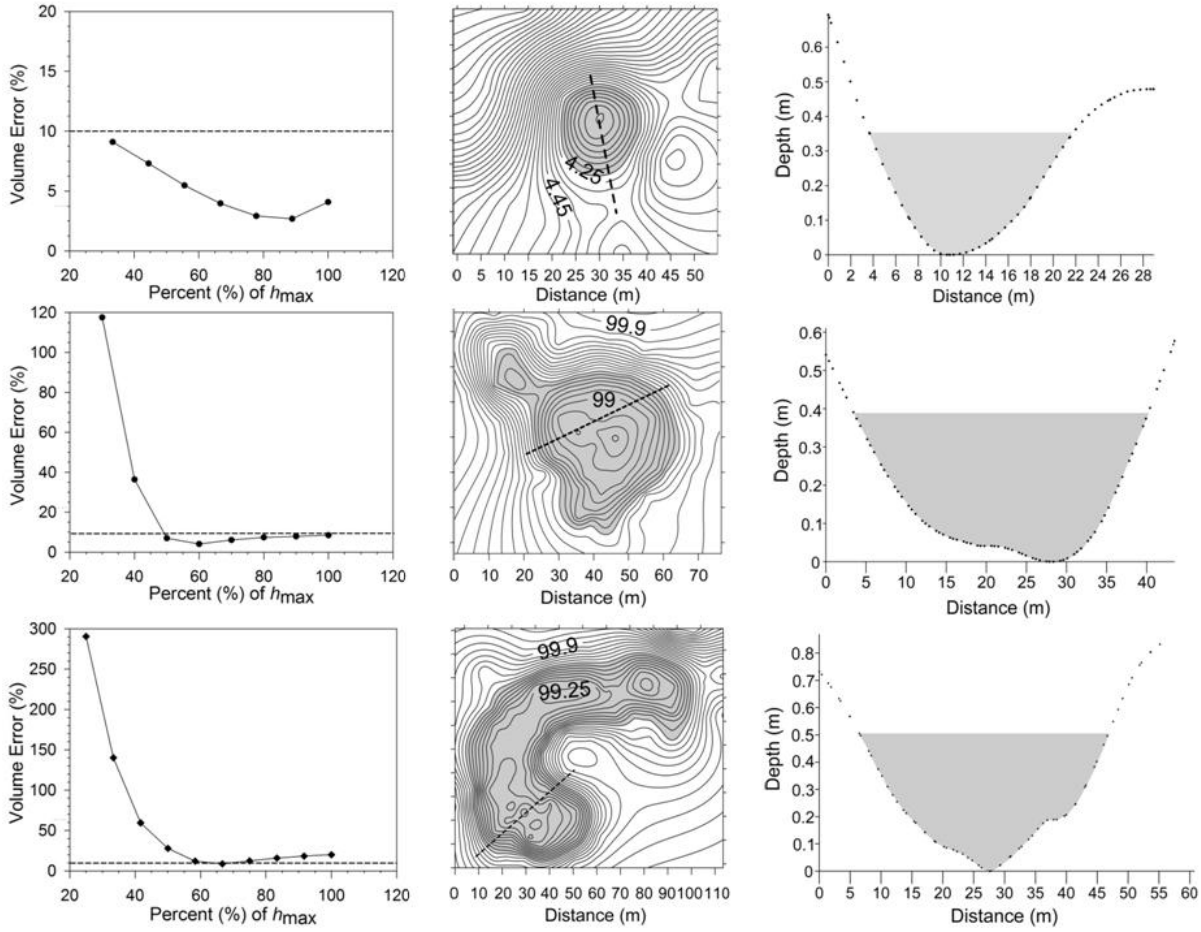

Figure 3.6. Results from analyzing the sensitivity of volume error to depth measurements. Graphs shown (left to right) are: the relationship between volume error and the depth at which A_2 is measured for the simplified *V-A-h* method; plan view of the wetland with 5 cm contours, illustrating the water level at ~80 of h_{max} shown in gray and the location of the cross section shown by the dashed line; and a cross section through the wetland illustrating the basin morphology. Wetlands used for this analysis were: a) D2 – regularly shaped morphology; b) W7 – semi-irregular morphology; c) W2 – irregular morphology.

3.2. Discussion

The full *V-A-h* method performed well when detailed survey data comprised many area and depth measurements. Volume estimates were not affected by wetland shape and area errors were within an acceptable range. Hayashi and van der Kamp (2000) found that survey-derived coefficients allowed for accurate estimations because depression characteristics were considered. Reliable performance of the full *V-A-h* method in this study and others (i.e., Brooks and Hayashi 2002, Carroll et al. 2005, Hill et al. 2006, Waiser 2006) confirms that the *V-A-h* coefficients can estimate volume well when considering wetlands to have a circular surface area and an approximately parabolic depression shape. This is true even when wetland morphology deviates from this approximation. For example, wetland S125 is the most irregularly shaped wetland in this study (see Figure 3.1 for shaded illustration) which is composed of two primary depressions (S125n and S125s) that connect when water level exceeds ~1.3 m. Despite the irregular morphology, the full *V-A-h* method still estimated volume within ~2% of actual. These results verify that the *V-A-h* equations are robust and can be applied to the range of wetland surface shapes present in the PPR.

Analysis of the simplified *V-A-h* method revealed that volume estimates were not consistently accurate when *s* and *p* were derived during drought conditions. Volume errors for several wetlands (B1, W1, W2, W4, W7, W9, and S92) were quite large (i.e., V_{err} > 20%). This is because the *s* and *p* coefficients are sensitive to basin morphology. This is illustrated by wetland W2 which shows an inconsistent rate of surface area increase relative to water depth across its storage capacity. Thus, the coefficients derived during drought conditions may not estimate volume of the entire depression well because an *A-h* range near h_{min} may not provide sufficient

data to accurately derive a *p* coefficient that characterizes the shape of the entire depression. The analysis of volume error sensitivity to depth measurements also illustrates that volume errors are highest when A_1 and A_2 are measured in drought-like conditions. Hayashi and van der Kamp (2000) developed their *V-A-h* equations for wetlands in smoothly shaped depressions. If the wetland is shallow and smoothly sloped (e.g., D2, Figure 3.6) then the coefficients derived during a drought period may represent the possible *A-h* range and estimate volume well. However, many prairie pothole wetlands differ significantly in their basin morphology, ranging from cone shaped to flat, pan-like depressions. If the wetland basin is discontinuous (i.e., has different rates of surface area increase with depth), or is irregular (e.g., W2, Figure 3.6) then coefficients derived during drought conditions should be limited to estimating volume for a range of area and depth that represents the conditions in which they were derived.

It is clear that correct timing of area and depth measurements for deriving *s* and *p* is important for estimating volume and area correctly. Deriving *s* and *p* from the simplified *V-A-h* method for average or wet conditions provided reasonably good estimates of volume and area. This is because the coefficients were derived from an *A-h* range that spanned the storage capacity of the wetland. Basin coefficients (*p*) derived from this method were a better approximation of the actual depression shape and thus provided a better estimation of storage. When using the average or wet conditions for a discontinuous wetland depression (W2) the volume errors were much lower than for drought-like conditions. Although the volume error was >10% for scenario 2 the depth analysis illustrated that lowering the depth for which A_2 is measured (Figure 3.6) would produce errors within the acceptable limit. Therefore, when applying the simplified *V-A-h* method the depth at which A_2 is measured should be less than h_{max}, ideally between 60-80% of h_{max}. When collecting two concurrent sets of area and depth measurements it would be ideal to

have a sufficient difference in depth between them so the range in storage capacity is captured. Practical guidelines for most wetlands (seasonal and semi-permanent) would involve a measurement of area and depth in spring when water levels are near ~70% of h_{max}, and a measurement of area and depth in late-summer before water levels are lower than 0.1 m. For deeper wetlands, it may be necessary to capture the water level fluctuations over multiple years when the water levels exhibit a declining or increasing trend.

In addition to considering when area and depth measurements, accurate measurements of the pond wetted perimeter and water depth are also essential for estimating volume correctly with the simplified *V-A-h* method. This analysis revealed that area measurements corresponding to the deepest water level are the most important perimeter to delineate correctly when using the simplified *V-A-h* method for average or wet conditions. Inaccurate measurements of A_2 caused the *s* coefficient, which represents area at h = 1 m, to have a maximum of 95% variation as compared to 40% variation of the *s* coefficient when A_2 was accurate. As a result, the estimated size of the wetland did not represent the actual wetland well and the volume estimation errors were greater. Figure 2.6 clearly shows how error could be introduced when delineating the wetted perimeter from an air photo. Therefore, measurement techniques that allow the wetted perimeter to be resolved with greater certainty are preferable (e.g., measuring wheel, GPS, low altitude air photos). Furthermore, since wetland ponds are fractal objects it is important to use a constant scale of measurement (i.e., step length) when collecting perimeter measurements. For example, using a constant distance of two meters between high-resolution GPS coordinates will ensure that perimeter measurements for different wetlands can be compared. Volume errors can be reduced if accurate methods are used such that the perimeter of the pond is delineated within ±1.5 m of actual. Sensitivity to perimeter delineation error will be less for larger ponds. Accurate

measurements of water depth are also important when using the simplified *V-A-h* method. Conly et al. (2004) reported that point measurements of water depth can be accurate to within 0.02 m. However, this accuracy can be compromised by soft wetland substrate, inconsistent measurement techniques, and by not measuring depth at the same location (Conly et al. 2004).

CHAPTER 4 – ESTIMATING WETLAND VOLUME USING A LIDAR DEM

4.1. Developing the LiDAR *V-A-h* Method

Previously, the Hayashi-van der Kamp *V-A-h* method had only been used to estimate wetland volume when a detailed topographic survey is available (Hayashi and van der Kamp 2000, Carroll et al. 2005, Hill et al. 2006, Waiser 2006). However, the theory outlined in section 2.5 has provided a framework for utilizing the simplified *V-A-h* method to estimate wetland volume from a LiDAR DEM. While the equations to estimate wetland depth and the *s* coefficient have been presented, there is still a need to develop a reliable process for extracting the wetland measurements (A_1, A_2, and Δh) required for the LiDAR *V-A-h* method. Therefore, the objective of this section was to use the study wetlands to develop the LiDAR *V-A-h* method. Section 4.1.1 outlines the measurement of surface area and Δh from LiDAR-derived elevation contours. Section 4.1.2 presents the process for selecting a *p* coefficient that will be used for estimating wetland depth, the *s* coefficient, and volume.

4.1.1. Elevation Contours

While LiDAR data collected over flat, bare ground provides relatively accurate measurements of elevation, open water causes problems for acquiring reliable LiDAR data. For example, laser pulses transmitted at an angle are often lost because water is highly reflective (Hopkinson 2006). This reduces the number of pulses available for calculating the water surface elevation. Furthermore, pulses that do return to the sensor may have partially penetrated the water surface causing inaccurate measurements of the water elevation. As a result, the water surface represented in the DEM may not provide reliable surface area measurements. Techniques

such as ‘filling’ the DEM could smooth the elevation values of the water surface and provide a more accurate area measurement. Research has also shown that ‘filling’ a DEM can provide surface area and depth measurements (Martz and De Jong 1988). However, the common GIS algorithm for ‘filling’ a DEM (Jenson and Domingue 1988) is time consuming for high resolution data (Planchon and Darboux 2001). Therefore, the technique of using elevation contours to measure surface area and changes in depth was developed for the LiDAR *V-A-h* method. This method utilizes DEM-derived elevation contours from the exposed portion of the wetland depression. These contours represent potential water surfaces that would occur when the wetland is filled with more water. Since LiDAR data collected from this portion of the depression provides a better measurement of elevation than the DEM water surface, these contours could provide reliable measurements for the LiDAR *V-A-h* method.

Elevation contours were created at 0.05 m intervals in ArcGIS from the bare-earth, 1-m resolution LiDAR-derived DEM. For each study wetland, the contours of interest were from the water surface to the point where water would spill from the depression (Figure 4.1). These contours were individually selected and exported to a new file. Each contour line was converted to a polygon so area could be calculated with the geometry function. Some contours could not be converted to polygons because the contour lines did not connect. To fix this problem, the ET GeoWizards toolset version 9.9 (ET Spatial Techniques, Pretoria, South Africa) was installed in ArcGIS and the ‘clean gap’ function was used to force the lines closed. When contours were closed they were converted to polygons and areas were calculated.

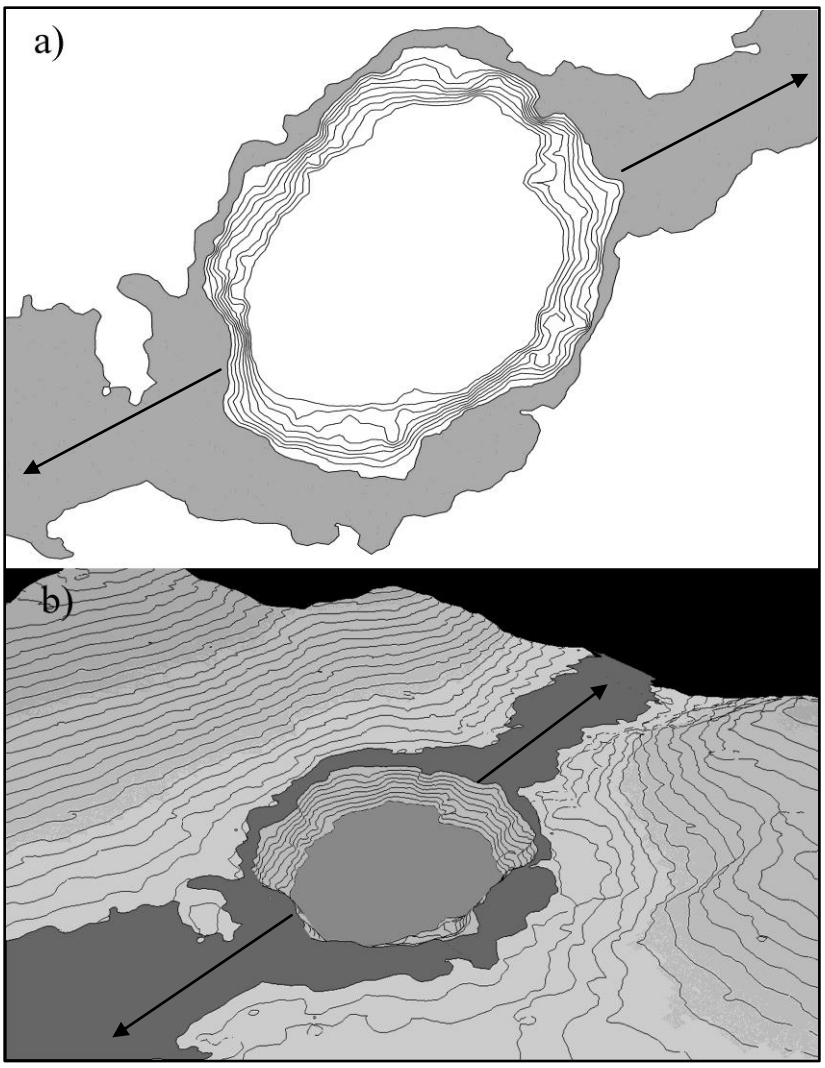

Figure 4.1. a) Plan view of wetland S104 in SDNWA with relevant, closed contours (white) and spill point contour (grey), b) Oblique view from above the DEM for wetland S104 with closed contours in the depression, spill point contour (shaded dark grey), and surrounding upland elevation contours. Arrows indicate spill flow direction.

4.1.2. Selecting the *p* Coefficient

To apply the simplified *V-A-h* method to LiDAR DEM data it is necessary to select a constant *p* coefficient for each wetland. Hayashi and van der Kamp (2000) suggested that a *p* value of 2.0 would likely represent seasonal wetlands with smooth depressions such as those found in SDNWA. However, wetlands across the PPR range from ephemeral to semi-permanent

with depressions resembling a range of shapes from cones to flat pans. Therefore, *p* values were determined from an average of the actual *p* values derived from the full *V-A-h* method (Table 3.1). In SCRB, three wetlands (W3, W8, and W10) had *p* values <1.5 which represents a depression similar to a cone. Therefore, a *p* value of 1.5 was used for these wetlands. The average *p* of the remaining eleven wetlands in SCRB was 1.83. In SDNWA, a *p* value of 2.0 adequately represented all of the wetlands except three (S90, S97, and S120). These three wetlands had an average *p* of 3.14 due to their pan-like shape (Hayashi and van der Kamp 2000).

Three wetlands (W1, W2, and S92) were selected to analyze the sensitivity of V_{err} to the *p* coefficient. These wetlands were chosen because they covered a range of maximum surface area (Appendix C) and they had a low V_{err} from the full *V-A-h* method (Table 3.1). The sensitivity analysis was accomplished by varying the *p* coefficient from 1.0 to 6.0 and calculating the *s* coefficient and V_{err}. The wetlands had a similar sensitivity to the *p* value, with V_{err} remaining below 15% when *p* was varied by ± 0.5 (Figure 4.2). This error was not caused by the *s* coefficient because it remained relatively stable across the *p* value range. V_{err} is thus likely due to the additional volume estimated when the depression bottom flattens and the sides become more steep (i.e., the *p* value increases).

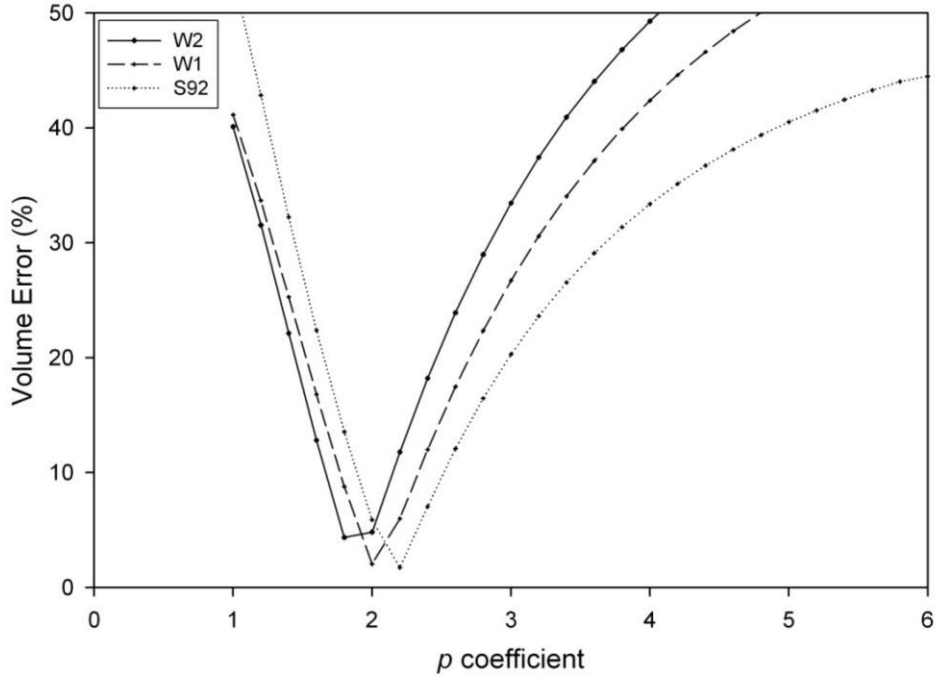

Figure 4.2. Sensitivity of volume error to the *p* coefficient illustrated for three wetlands (W1, W2, S92). The *p* coefficient was varied from 1.0 to 6.0 and used to estimate the average *s* coefficient and the V_{err}.

4.2. Automation of the LiDAR *V-A-h* Method

The data collection process described above was automated so the necessary data for volume estimation could be rapidly acquired for multiple wetlands. An ArcGIS model (Figure 4.3) was built to extract elevation and area data. Input data for the model were the LiDAR DEM and a GIS file that delineates the extent of each wetland. The model has five main steps: 1) Contours are created at 0.05 m intervals from the LiDAR DEM. 2) The wetland extents are buffered and used to clip the contours so only the relevant data are analyzed. 3) The contour data are split into a separate file for each wetland based on the buffered wetland extent. 4) Contour lines were forced closed (if necessary) and converted to a polygon format so that area can be

calculated. 5) The elevation and area data are exported to a Microsoft Excel dBase format spreadsheet.

A Visual Basic script was created to automate the calculations necessary for the LiDAR *V-A-h* method (Appendix D). There are six main steps to the script: 1) The dBase file is opened in Microsoft Excel for analysis. 2) Unnecessary columns of data added during the GIS processing are deleted, leaving only the elevation and area data. 3) Data are sorted by surface area from largest to smallest. The script then prompts the user to enter the minimum surface area to be retained for analysis. All rows of data containing smaller area measurements are deleted. 4) The user is prompted to enter the *p* coefficient. 5) The elevation and area data are arranged so that every possible combination of A_1 and A_2 is used to calculate an *s* coefficient. 6) Volume and area are estimated at 0.05 m depth increments using the average *s* coefficient. V_{max} is reached at the depth where the estimated area equals the contour-derived A_{max}.

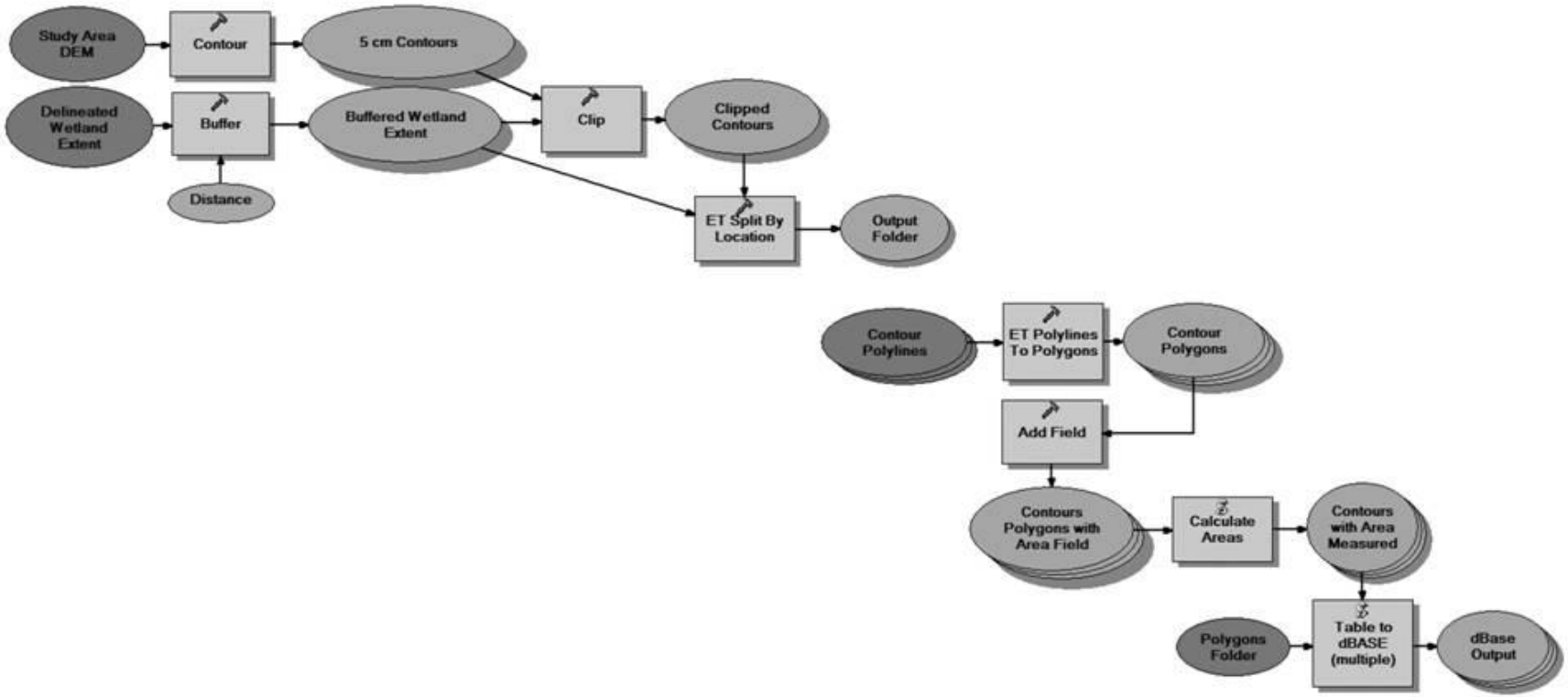

Figure 4.3. ArcGIS model built to analyze the LiDAR DEM and extract elevation and area data. See text for description of the main steps in the model.

4.3. Assessing Volume Error for the Study Wetlands

Volumes estimated by the LiDAR *V-A-h* method for 26 study wetlands (excluding S125s) were compared to the actual volumes. Because wetland S125s was indistinguishable from S125n, they were analyzed together as S125n&s. Since the topography varied between sites and LiDAR data were collected in different years, different numbers of area measurements were extracted from each wetland (Table 4.1). For example, the topographic slope is greater in SDNWA which allowed for many more area measurements to be extracted from the DEM. By contrast, the topographic slope for SCRB is less pronounced and the LiDAR data were collected after a series of wet years. Consequently, the ponds were relatively full and fewer area measurements could be extracted. Depending on how many area measurements were obtained from the DEM there were either one or multiple *s* coefficients calculated for each wetland (Table 4.1). When using the automated method, the Visual Basic script was able to generate every possible *s* coefficient near-instantaneously. For each wetland there was an *s* coefficient that was most accurate and produced the lowest V_{err} (Figure 4.4a). However, when the actual wetland volumes are not known it is not possible to identify the most accurate *s* coefficient. Therefore, every possible combination of A_1 and A_2 were analyzed and the average *s* coefficient was used to estimate volume. The average volume error was 20%, ranging from 2% to 52% (Figure 4.4b). While V_{err} was <10% for 7 wetlands, there were 12 wetlands with 10-25% V_{err}, and 7 wetlands with >25% V_{err}.

Table 4.1. Number of area measurements and s coefficients generated by the Visual Basic script from the automated LiDAR analysis

Wetland ID	# of *A* measurements	# of *s* coefficients	Wetland ID	# of *A* measurements	# of *s* coefficients
Smith Creek			St. Denis		
B1	4	6	D1	5	10
LR2	4	6	D2	12	66
LR3	12	66	D3	18	153
LR4	5	10	S1	4	6
LR7	2	1	S104	9	36
W1	5	10	S109	17	136
W2	2	1	S120	11	55
W3	2	1	S124	9	36
W4	2	1	S125n&s	12	66
W7	2	1	S90	50	1275
W8	6	15	S92	20	190
W9	6	15	S97	8	28
W10	6	15			
W11	2	1			

An analysis of *s* coefficient variation was then conducted to provide insight into why some wetlands had a high volume error. For each wetland, the range in *s* coefficient was calculated and expressed as the percent deviation from the actual *s* coefficient. This allowed for the *s* coefficient range to be compared among wetlands. Wetlands with <25% volume error were combined for analysis because a natural break occurred between 25% and 32%. This group of wetlands had a range of estimated *s* coefficients from +19 to -16%. While wetlands with 25-52% volume error had an *s* coefficient range from +43 to -98%. A regression analysis revealed a moderate but statistically significant relationship exists between *s* coefficient range and the V_{err} ($r^2 = 0.40$, P = 0.0047). This indicates that wetlands with a high V_{err} also have a large range in the estimated *s* coefficient. To understand the cause of this variation it was necessary to investigate the area measurements because these data represent the depression characteristics. Therefore, the difference in surface area between consecutive elevation contours was calculated for each

wetland. There was a strong, positive statistical relationship between the average difference in surface area for each wetland and the *s* coefficient (Figure 4.5). This means wetlands with a large volume error (e.g., W9, S124, S109, and LR3) have a large range in the *s* coefficient and a large average difference in area between contours. Such depressions have abrupt, large increases in area between contours that indicate the depression morphology changes suddenly. Thus, these wetlands have depression profiles that are not smooth, but are discontinuous. Since the data collected from these depressions were so variable, using an average *s* produced a relatively high V_{err} for these wetlands. This analysis provides valuable insight for determining the extent of V_{err} when using the LiDAR *V-A-h* method. For example, wetlands with a small range in the estimated *s* coefficients are likely to provide a better estimate of volume for any given set of area measurements.

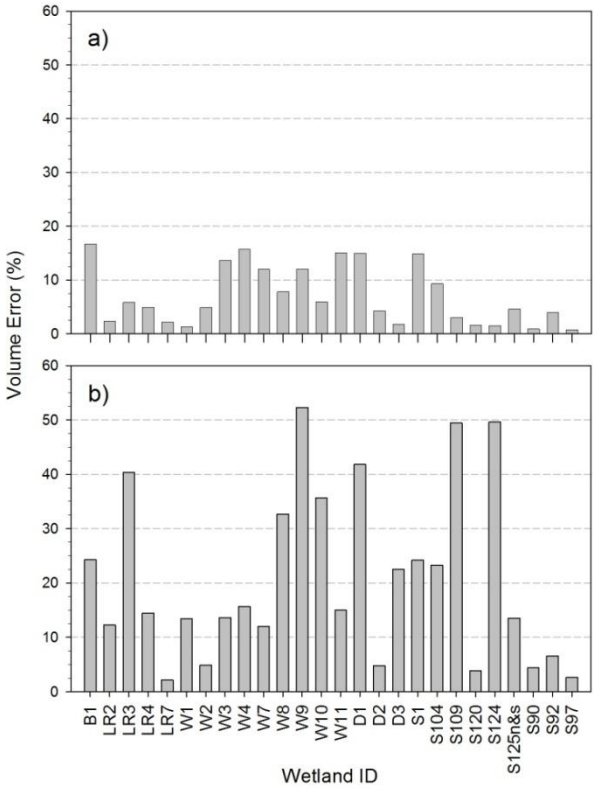

Figure 4.4. Volume error produced by using a) the LiDAR *V-A-h* method; b) an average *s* coefficient in the LiDAR *V-A-h* method.

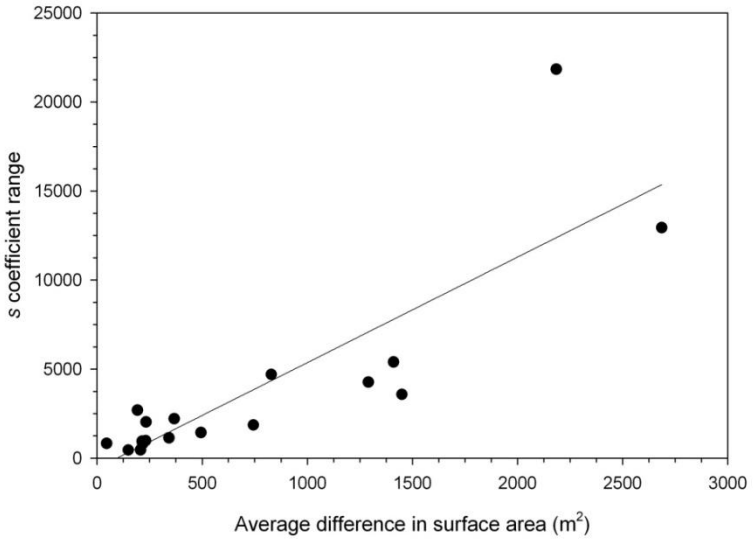

Figure 4.5. Comparing the average difference in surface area to the *s* coefficient range indicating a strong statistical relationship ($r^2 = 0.71$, P = 0.0001). Since S90 and LR3 had very large values they were identified as outliers with the studentized residuals test (>±2.5) and were removed prior to statistical analysis.

4.4. Comparing the LiDAR *V-A-h* Method to *V-A* Equations

Maximum volume estimated by the LiDAR *V-A-h* method was, on average, more accurate than that estimated through the Wiens (2001) and Gleason et al. (2007) *V-A* equations (Figure 4.6). When comparing the estimated volume to the actual, the Wiens equation (Eq. 2.10) consistently underestimated V_{max}. This discrepancy was most severe for the large wetlands at both sites (Figure 4.6b and d). Since the equation was developed for the Upper Assiniboine River Basin, of which SCRB is a sub-basin, it seems that the regression equation does not characterize the rolling morainal topography of SDNWA. Despite that Gleason's equations (Eq. 2.11 - 2.13) were developed specifically for each physiographic region in the PPR, the Prairie Coteau (Eq. 2.12) equation estimated volume most accurately for both sites. This was the case even though the topography was relatively flat at SCRB and hummocky and rolling at SDNWA. With this

equation, the volumes of small wetlands were consistently underestimated (Figure 4.6a and c). However, volumes of larger wetlands (i.e., ~4,500 m^3) were estimated quite well by Gleason's equations (Figure 4.6b and d).

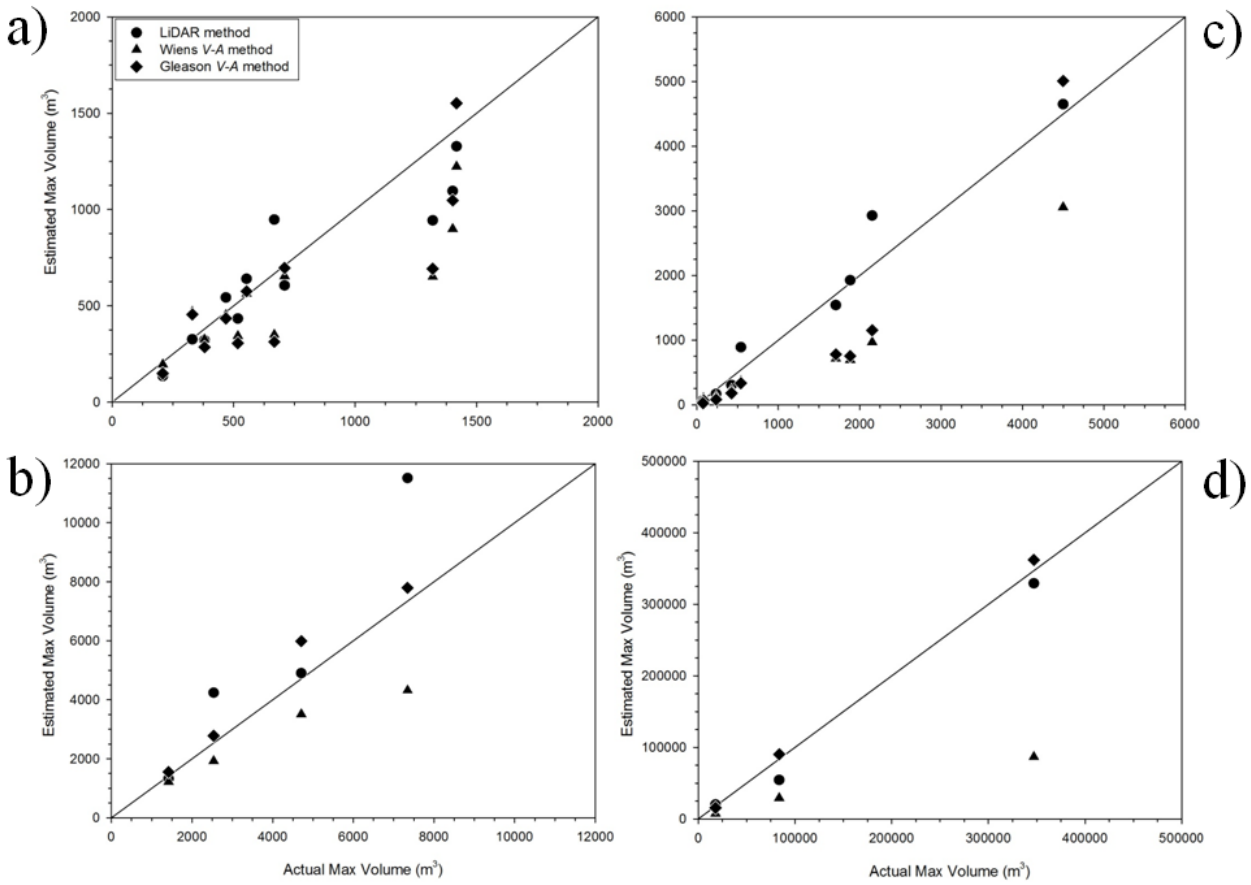

Figure 4.6. Volume estimated through the LiDAR *V-A-h*, Wiens and Gleason methods for a) SCRB small and b) SCRB large wetlands; c) SDNWA small and d) SDNWA large wetlands.

4.5. Case Study

The automated LiDAR *V-A-h* method was implemented at SDNWA to test its performance and assess if the model could be used to accurately estimate storage at a large spatial scale. Model set-up was completed through the following steps: 1) The LiDAR DEM and

the GIS file containing the delineated wetland extents were selected as input (Figure 4.7); 2) a buffer distance of 35 m was selected so that all relevant contours were included; 3) the contour files for each wetland were selected so the model could run in batch mode; and 4) the output filename for each polygon was specified manually. Fifty-eight wetlands were identified from the air photo and used for this analysis. The GIS model took approximately 70 minutes to process for the entire study site, with the majority of time needed to split the contour data by wetland location. The Visual Basic script was implemented from a blank spreadsheet that was located in the same folder as the dBase files. The code was modified to contain the current folders' pathname so the script would be able to identify the spreadsheets to open and analyze. When running the script the first dBase file was opened, the user was asked for the smallest surface area measurement to keep and the *p* coefficient, the new columns of data were generated, and then the user was prompted to save the file. On average, each spreadsheet was analyzed in ~10 seconds. If anomalous contour data were encountered the script would stop and the file was deleted manually. This was the case for three wetlands (D1, S86 and S134) because the contour data were incomplete. Of the thirteen wetlands with actual volume data, three were not analyzed (D1, S125s and S1). Pond S1 was excluded because of an island present in the middle, which required manual processing. Pond S125s and S125n were analyzed as one wetland (S125n&s).

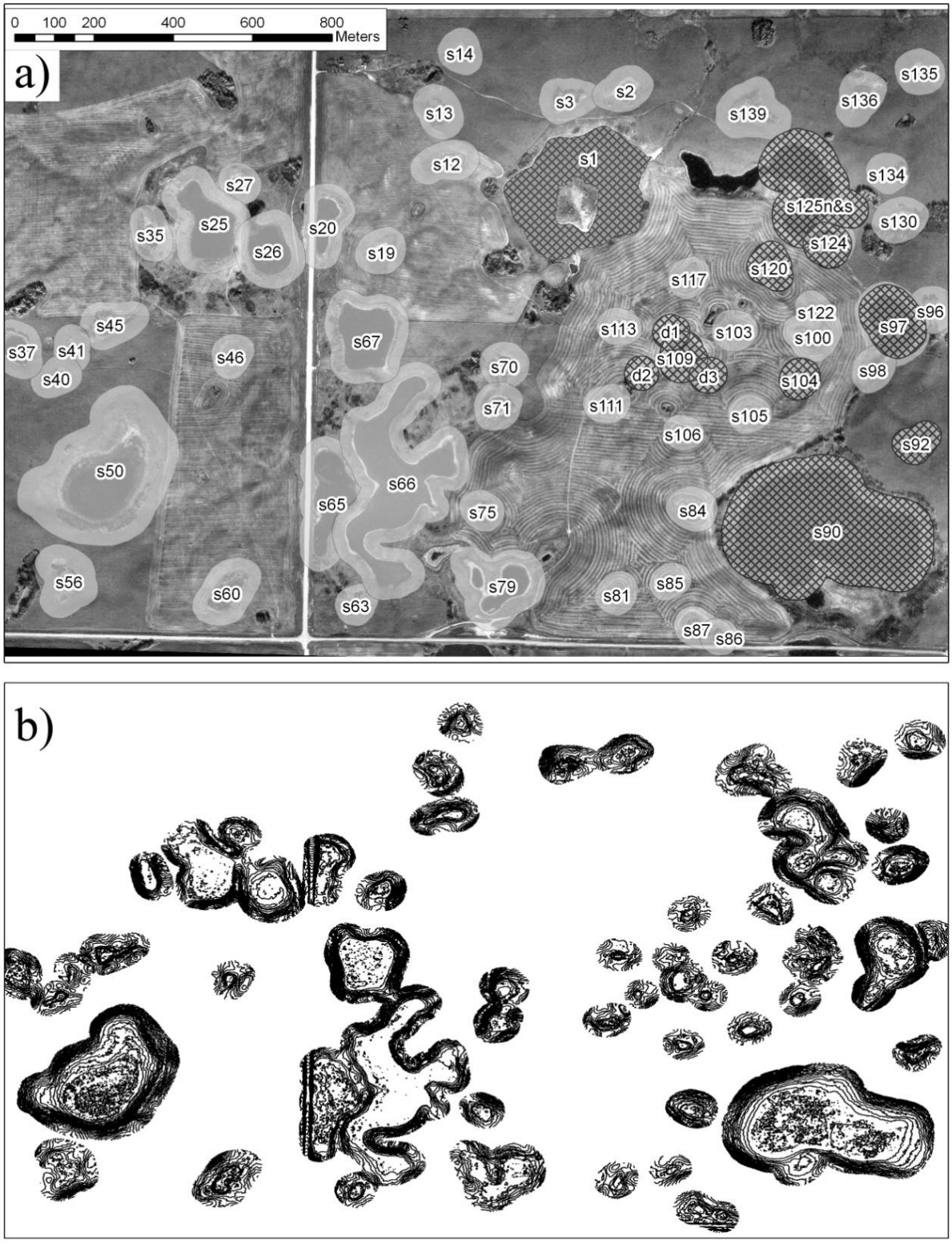

Figure 4.7. SDNWA study site: a) air photo (1997) with wetlands delineated and buffered. Wetlands with actual volumes indicated by cross-hatching; b) elevation contours derived from LiDAR DEM (5 m contours shown for display purposes)

Volume estimates from the automated method (Table 4.2 & 4.3) were slightly different than those computed manually (section 4.3). Although the same *p* values were used, the automated method usually extracted a different number of area measurements than were extracted manually, and thus the average *s* coefficients differed slightly. For most wetlands, volume estimates were very similar to the manual LiDAR *V-A-h* method, with the exception of wetland S109. The volume RMS error for S109 was higher than that reported in section 4.4 because the average *s* coefficient was overestimated. This occurred because area measurements were extracted to a deeper depth which allowed for larger area measurements to be incorporated when the *s* coefficient was calculated.

Table 4.2. Results from the automated LiDAR *V-A-h* method for wetlands with survey data.

Wetland ID	*p* coefficient	*s* coefficient	*h*	A_{max} (m^2)	V_{max} (m^3)
D2	2.00	1041	0.45	470	105
D3	2.00	661	0.7	460	160
S90	3.14	70635	3.4	154000	319880
S92	2.00	2143	1.2	2570	1540
S97	3.14	13645	0.7	10870	4650
S104	2.00	1664	0.7	1160	410
S109	2.00	4733	1.2	5680	3400
S120	3.14	2653	1.1	2820	1890
S124	2.00	4748	0.6	2850	850
S125n&s	2.00	12768	1.8	23780	21400

An additional difference was that V_{max} estimated through the automated method rarely corresponded with the actual V_{max} from the survey-derived DEM. For seven wetlands, V_{max} was much larger, and h_{max} was deeper, when using the automated method. However, for three wetlands, V_{max} was smaller than the survey-derived V_{max}. The reason for a larger V_{max} is that it was based on the largest A measurement obtained from the contour analysis, whereas the actual V_{max} was based on the extent of the wetland from the survey-derived DEM. As a result the automated method extracted more surface area measurements and estimated a deeper depth and larger volume. The smaller V_{max} was likely caused by inadequate closed contours at the deepest depths. Since the estimated V_{max} rarely corresponded with the actual V_{max}, the volumes reported (Table 4.2) correspond to the h_{max} from the topographic survey-derived DEM (Appendix C).

Table 4.3. Case study results from the automated LiDAR *V-A-h* method for wetlands without survey data.

Wetland ID	*p* coefficient	*s* coefficient	h_{max}	A_{max} (m^2)	V_{max} (m^3)
S2	2.00	5049	1.2	5820	3360
S3	2.00	1086	0.9	1020	480
S12	2.00	2349	1.5	3460	2540
S13	2.00	2718	1.7	4540	3790
S14	2.00	1836	0.9	1660	750
S19	2.00	1979	1.2	2440	1500
S20	2.00	10566	0.5	5690	1530
S25	2.00	24886	0.8	19790	7870
S26	2.00	6499	1.8	11440	10080
S27	2.00	4892	0.5	2340	560
S35	2.00	3057	1.0	2900	1380
S37	2.00	4868	0.7	3480	1250
S40	2.00	1122	1.2	1310	760
S41	2.00	3296	0.9	2820	1200
S45	2.00	2196	1.1	2360	1270
S46	2.00	2448	0.7	1600	520
S50	2.00	10521	7.6	79780	302470
S56	2.00	10077	0.8	8440	3540
S60	2.00	4872	1.3	6270	4030
S63	2.00	1681	1.4	2400	1720
S65	2.00	34363	0.7	22900	7640
S66	2.00	39688	1.5	60850	46650
S67	2.00	6867	3.2	21780	34530
S70	2.00	1411	2.1	2960	3100
S71	2.00	5307	0.5	2890	790
S75	2.00	2310	1.3	3020	1980
S79	2.00	46598	0.3	13400	1930
S81	2.00	2105	0.9	1840	800
S84	2.00	2130	1.0	2140	1080
S85	2.00	3373	0.5	1560	360
S87	2.00	1072	0.2	230	25
S96	2.00	1830	0.3	600	100
S98	2.00	4316	0.4	1600	300
S100	2.00	1055	1.0	1100	570
S103	2.00	1642	1.3	2100	1340
S105	2.00	1673	1.3	2230	1480
S106	2.00	1746	1.5	2550	1870
S111	2.00	1528	0.9	1380	620
S113	2.00	766	1.2	930	560
S117	2.00	2316	0.8	1900	790
S122	2.00	1018	0.9	910	400
S130	2.00	4346	1.1	4970	2850
S135	2.00	2616	1.0	2660	1350
S136	2.00	2452	0.6	1560	500
S139	2.00	3906	1.0	3850	1900

4.6. Strengths and Limitations of the LiDAR *V-A-h* Method

This chapter has demonstrated that the simplified *V-A-h* method can be used along with LiDAR DEM-derived wetland characteristics to estimate wetland storage. The LiDAR *V-A-h* method is advantageous because wetland storage can be estimated for broad spatial extents without visiting individual wetlands. Furthermore, the automated method can reduce the time required to extract the wetland information necessary to apply the simplified *V-A-h* method. This eliminates the time and money required to maintain water level measurements or to collect a detailed topographic survey. A comparison between methods demonstrated that the LiDAR *V-A-h* method outperforms two sets of *V-A* regression equations (Wiens 2001, Gleason et al. 2007) currently available for the PPR. Further improvements to the automated method could be made to incorporate an algorithm that would identify the smallest relevant surface area to retain. This would reduce the amount of user input and speed the processing time.

However, there are limitations to the method. Since the simplified *V-A-h* method relies on having two area and depth measurements, the user must be able to extract multiple closed contours from the DEM. While these are easily extracted from a deep or dry depression, closed contours are difficult to extract when the topography is relatively flat, the wetland is full of water, or the topography has been altered by a drainage ditch. For example, in trials of the method on quarter-sections in SCRB it was common to extract none or only one contour line that represents a potential water surface because the topography is quite flat, the LiDAR was flown after a series of wet years, and the topography is severely affected by wetland drainage. When this situation occurs the LiDAR method cannot be used to estimate volume. In contrast, the SDNWA case study was more ideal for applying the method because the topographic slope was greater than SCRB so it was possible to extract more area measurements before the spill point of

the wetland was reached. To overcome these issues, LiDAR data should be acquired in dry years for watersheds in the PPR when pond water levels are close to h_{min}. As well, data acquisition is also desirable in late fall when there is less vegetation to prevent the LiDAR pulses from reaching the ground. This produces a DEM with a better vertical accuracy because there are more LiDAR pulses used to calculate elevation (Töyrä et al. 2006).

Another consideration regarding LiDAR data collection is the cost. LiDAR is relatively expensive and may not be suitable for all research or water resource management projects. While the cost is likely prohibitive for small scale projects, LiDAR data are increasingly being utilized for hydrological research across North America (Hopkinson and Pietroniro 2006). The cost may be a worthwhile investment for regional projects, as recent modeling exercises have shown that accurate estimation of wetland storage is critical for reliable prediction of streamflow in the PPR (Fang and Pomeroy 2008, Fang et al. submitted). Thus, having high quality topographic data could eliminate the need for expensive field visits.

CHAPTER 5 – CONCLUSIONS

My first research objective was to determine how surface area shape influences estimates of wetland volume through the Hayashi-van der Kamp *V-A-h* method. A shape analysis of wetlands in SCRB and SDNWA revealed that the survey-derived, full *V-A-h* method estimates volume and area extremely well regardless of surface area shape. The *V-A-h* equations are therefore robust and applicable to the range of surface area shapes observed in the PPR. The second component of this objective was to create guidelines for applying the less data-intensive, simplified *V-A-h* method. Analysis of the simplified *V-A-h* methods revealed that the depression (*p*) and size (*s*) coefficients are sensitive to the timing of *A-h* measurements. When using area and depth measurements derived during drought conditions the errors were high for wetlands that do not have regularly-shaped basins. This is because the coefficients do not fully represent the *A-h* range of the wetland. Therefore, the simplified method should not be parameterized for irregular depressions during drought conditions. The *A-h* combination for average or wet conditions produced accurate estimates of volume (error <10.5%) because most of the storage capacity was considered. This analysis also demonstrated the importance of measuring the wetted perimeter of the deepest water level accurately to have volume errors less than 10%. Measurements of area and depth should be collected concurrently in the spring, when water levels are near ~70% of h_{max}, and again later in the year prior to water levels <0.1 m. For permanent wetlands it may not be possible to measure surface areas near h_{min} or h_{max} in one year, therefore *A-h* measurements should be collected over ~3-4 years to obtain measurements during periods of strongly fluctuating water levels. Application of the simplified *V-A-h* method in conjunction with the above guidelines will permit accurate storage estimation at the scale of multiple wetlands.

The second objective of this research was to determine if the *V-A-h* coefficients could be extracted from a LiDAR-derived DEM, and used to estimate volume. While total wetland depth cannot be measured directly from the LiDAR DEM, multiple area measurements and the change in depth between them can be extracted through a simple GIS analysis of the DEM. If a constant *p* value is assumed then the depth of water at the time of LiDAR data acquisition can be calculated. With a measurement of water depth the *s* coefficient can be calculated and used in the simplified *V-A-h* method to estimate volume. Estimates of V_{max} from these data outperformed estimates generated with the *V-A* equations (Wiens 2001, Gleason et al. 2007). This was likely due to the inclusion of information on depression morphology when calculating volume with the DEM.

The second component of this objective was to determine if the process to retrieve the coefficients from a LiDAR DEM could be automated and wetland storage could be estimated at a large spatial scale. A GIS model and Visual Basic script were created to automatically extract the elevation and area data necessary for use in the LiDAR *V-A-h* method. Although the model still requires user input, such as the minimum area to retain and the *p* coefficient, the process to retrieve the data is quite fast and allows for a large area to be analyzed in a short period of time. The SDNWA case study illustrated that the LiDAR *V-A-h* method can be applied to a small prairie watershed to accurately predict wetland water storage. Reducing the amount of user input would likely speed up the analysis and make this GIS based method for estimating volume easier to apply.

Overall, the results from this thesis have shown that the Hayashi-van der Kamp *V-A-h* equations are a robust method for estimating wetland water storage volumes across varying topographies in the PPR, even with various data sources. While the full *V-A-h* method has only

been used at the scale of individual wetlands (Carroll et al. 2005, Hill et al. 2006, Waiser 2006), the *V-A-h* methods developed here can be applied at broader spatial scales. The simplified *V-A-h* method can provide a less time-intensive method for modelling and understanding ecological functions of wetlands, such as vegetation dynamics (Poiani et al. 1996) and water quality (Waiser 2006). The LiDAR *V-A-h* method, which outperformed two common *V-A* equations (Wiens 2001, Gleason et al. 2007), was automated and applied to the entire SDNWA. Therefore, the LiDAR *V-A-h* method can be used to quantify the capacity of prairie wetlands to store surface water. This has assisted in creating an improved prediction of streamflow in a prairie watershed (Pomeroy et al. 2009). Results could also be used to better understand the impact of natural and artificial wetland drainage on streamflow response by predicting volume of wetland discharge to streamflow. Therefore, the methods developed in this thesis will allow future researchers and water managers to more accurately characterize wetland hydrology in the PPR.

REFERENCES

Brinson, M.M. 1993. A hydrogeomorphic classification for wetlands. Wetlands Research Program Technical Report WRP-DE-4. US Army Corps of Engineers, Waterways Experiment Station, Vicksburg, Mississippi, 103 pp.

Brooks, R.T. and M. Hayashi. 2002. Depth-area-volume and hydroperiod relationships of ephemeral (vernal) forest pools in southern New England. Wetlands 22:247-255.

Carroll, R., G. Pohll, J. Tracy, T. Winter, and R. Smith. 2005. Simulation of a semi-permanent wetland basin in the Cottonwood lake area, East-Central North Dakota. Journal of Hydrologic Engineering 10:70-84.

Conly, F., M. Su, G. van der Kamp, and J. B. Millar. 2004. A practical approach to monitoring water levels in prairie wetlands. Wetlands 24:219-226.

Cressie, N. 1990. The origins of Kriging. Mathematical Geology 22:240-252.

Elliott, J. A. and A. A. Efetha. 1999. Influence of tillage and cropping system on soil organic matter, structure and infiltration in a rolling landscape. Canadian Journal of Soil Science 79:457-463.

Fang, X. And J. W. Pomeroy. 2007. Snowmelt runoff sensitivity analysis to drought on the Canadian prairies. Hydrological Processes 21:2594-2609.

Fang, X. and J. W. Pomeroy. 2008. Drought impacts on Canadian prairie wetland snow hydrology. Hydrological Processes 22:2858-2873.

Fang, X. J. W. Pomeroy, C. J. Westbrook, X. Guo, A. G. Minke, and T. Brown. Submitted. Prediction of snowmelt derived streamflow in a wetland dominated prairie basin. Hydrology and Earth System Sciences.

Forman, R. T. T., and M. Godron. 1986. Landscape Ecology. John Wiley & Sons, New York, USA.

Gleason, R. A., B. A. Tangen, M. K. Laubhan, K. E. Kermes, and N. H. Euliss. 2007. Estimating water storage capacity of existing and potentially restorable wetland depressions in a subbasin of the Red river of the north. U.S. Geological Survey, U.S. Department of the Interior Open-file report 2007-1159.

Gleason, R. A., B. A. Tangen. 2008. Floodwater storage. *In* R. A. Gleason, M. K. Laubhan, N. H. Euliss, Jr. (ed.) Ecosystem services derived from wetland conservation practices in the United States prairie pothole region with an emphasis on the U.S. Department of Agriculture

Conservation Reserve and Wetlands Reserve Programs. Professional Paper 1745, U.S. Geological Survey, Reston, VA.

Goodwin, R. B. and F. R. J. Martin. 1975. Calculation of gross and effective drainage areas for the Prairie Provinces. In: Canadian Hydrology Symposium - 1975 Proceedings, 11-14 August 1975, Winnipeg, Manitoba. Associate Committee on Hydrology, National Research Council of Canada, pp. 219-223.

Gray, D. M., P. G. Landine, and R. J. Granger. 1985. Simulating infiltration into frozen prairie soils in streamflow models. Canadian Journal of Earth Sciences 22:464-472.

Gusman, A. J., R. L. Voigt, and S. M. Forman. 2001. Delineation and classification of prairie pothole wetlands using GIS and aerial photos. Wetlands Engineering & River Restoration 34:doi 10.1061/40581(2001)88.

Haan, C. T. and H. P. Johnson. 1967. Geometric properties of depressions in north-central Iowa. Iowa State Journal of Science 42:149-160.

Hayashi, M., G. van der Kamp, and D. L. Rudolph. 1998. Water and solute transfer between a prairie wetland and adjacent uplands, 1. Water balance. Journal of Hydrology 207:42-55.

Hayashi, M. and G. van der Kamp. 2000. Simple equations to represent the volume-area-depth relations of shallow wetlands in small topographic depressions. Journal of Hydrology 237:74-85.

Hayashi, M., G. van der Kamp, and R. Schmidt. 2003. Focused infiltration of snowmelt water in partially frozen soil under small depressions. Journal of Hydrology 270:214-229.

Hill, A. J., V. S. Neary, and K. L. Morgan. 2006. Hydrologic modeling as a development tool for HGM functional assessment models. Wetlands 26:161-180.

Hopkinson, C. 2006. An overview of airborne laser scanning technology. In: Hydroscan: Airborne laser mapping of hydrological features and resources. Edited by: Chris Hopkins, Alain Pietroniro and John Pomeroy. Papers presented at: Hydroscan Conference, 22 September 2006, Saskatoon, Saskatchewan.

Hopkinson, C. and A. Pietroniro. 2006. Hydrological applications of airborne laser scanning. In: Hydroscan: Airborne laser mapping of hydrological features and resources. Edited by: Chris Hopkins, Alain Pietroniro and John Pomeroy. Papers presented at: Hydroscan Conference, 22 September 2006, Saskatoon, Saskatchewan.

Hubbard, D. and R. L. Linder. 1986. Spring runoff retention in prairie pothole wetlands. Journal of Soil and Water Conservation 41:122-125.

Huel, D. 2000. Managing Saskatchewan Wetlands: A landowner's guide. Saskatchewan Wetland Conservation Corporation, Regina, Canada. 69 pp.

Jenson, S . K. and J. O. Domingue. 1988. Extracting topographic structure from digital elevation data for geographic information systems analysis. Photogrammetric Engineering and Remote Sensing 54:1593-1600.

Johnson, W. C., B. V. Millett, T. Gilmanov, R. A. Voldseth, G. R. Guntenspergen, and D. E. Naugle. 2005. Vulnerability of northern prairie wetlands to climate change. Bioscience 55:863-872.

LaBaugh, J. W., T. C. Winter, and D. O. Rosenberry. 1998. Hydrologic functions of prairie wetlands. Great Plains Research 8:17-37.

Legleiter, C. J., D. A. Roberts, and R. L. Lawrence. 2009. Sprectrally based remote sensing of river bathymetry. Earth Surface Processes and Landforms. 34:1039-1059.

Lindsay, J. B. and I. F. Creed. 2004. Drainage basin morphometrics for depressional landscapes. Water Resources Research 40:W09307, doi:10.1029/2004WR003322, 2004.

Liu, H. and L. Wang. 2008. Mapping detention basins and deriving their spatial attributes from airborne LiDAR data for hydrological applications. Hydrological Processes 22:2358-2369.

Ludden A. P., D. L. Frink, and D. H. Johnson. 1983. Water storage capacity of natural wetland depressions in the Devils Lake basin in North Dakota. Journal of Soil and Water Conservation 38:45-48.

Mandelbrot, B. 1967. How long is the coast of Britain? Statistical self-similarity and fractional dimension. Science 156:636-638.

Manitoba Conservation, Environment Canada, Sask Water, 2000. Upper Assiniboine River Basin Study, Main Report. Manitoba, 125 pp.

Martz, L. W. and E. De Jong. 1988. CATCH: A FORTRAN program for measuring catchment area from a digital elevation model. Computers & Geosciences 14:627-640.

McGarigal, K. and B. Marks. 1995. FRAGSTATS: Spatial pattern analysis program for quantifying landscape structure. U.S. Department of Agriculture, Forest Service, Portland, Oregon, USA. PNW-GTR-351.

Meyboom, P. 1966. Unsteady groundwater flow near a willow ring in hummocky moraine. Journal of hydrology 4:38-62.

Millar, J. B. 1971. Shoreline-area ratios as a factor in rate of water loss from small sloughs. Journal of Hydrology 14:259-284.

Miller, J. J., D. F. Acton, and R. J. St. Arnaud. 1985. The effect of groundwater on soil formation in a morainal landscape in Saskatchewan. Canadian Journal of Soil Science 65:293-307.

Mitsch, W. J. and J. G. Gosselink. 1993. Wetlands. 2nd Edition. Van Nostrand Reinhold, New York. 722 pp.

National Wetlands Working Group. 1988. Wetlands of Canada. Ecological Land Classification Series, No. 24. Environment Canada, Sustainable Development Branch, Ottawa, Ontario, Canada, and Polyscience Publications Inc., Montréal, Quebec, Canada.

Ogaard, L. A., J. A. Leitch., D. F. Scott, and W. C. Nelson. 1981. The fauna of the prairie wetlands: research methods and annotated bibliography. North Dakota State University, Agricultural Experiment Station, Fargo, North Dakota, USA. Research Report No. 86.

Parkhurst, R. S., T. C. Winter, D. O. Rosenberry, and A. M. Sturrock. 1998. Evaporation from a small prairie wetland in the Cottonwood Lake area, North Dakota - An energy-budget study. Wetlands 18:272-287.

Parsons, D. F., M. Hayashi, and G. van der Kamp. 2004. Infiltration and solute transport under a seasonal wetland: bromide tracer experiments in Saskatoon, Canada. Hydrological Processes 18:2011-2027.

PFRA, 2008. Prairie Farm Rehabilitation Association Watershed Project, Sub-Basin Delineation, Version 8.

Planchon O. and F. Darboux. 2001. A fast, simple and versatile algorithm to fill the depressions of digital elevation models. Cantena 46:159-176.

Poiani, K. A., W. C. Johnson, G. A. Swanson, and T. C. Winter. 1996. Climate change and northern prairie wetlands: simulations of long-term dynamics. Limnology and Oceanography 41:871-881.

Pomeroy, J. W. and D. M. Gray. 1995. Snowcover Accumulation, Relocation, and Management. NHRI Science Report No. 7, Environment Canada, Saskatoon., 144 pp.

Pomeroy, J. W., D. de Boer, and L. W. Martz. 2007. Hydrology and water resources. *In* Thraves, B., Lewry, M.L, Dale, J.E. and Schlichtmann, H. (Eds.). Saskatchewan: Geographic Perspectives. Regina: CRRC, 63-80.

Pomeroy, J., X. Fang, C. Westbrook, A. Minke, X. Guo, and T. Brown. 2009. Prairie hydrological model study final report, December 2009. Centre for Hydrology report no. 7. 114 pp.

Price, J. S. 1993. Water level regimes in prairie sloughs. Canadian Water Resources Journal 18:95-105.

Rosenberry, D. O. and T. C. Winter. 1997. Dynamics of water-table fluctuations in an upland between two prairie-pothole wetlands in North Dakota. Journal of Hydrology 191: 266-289.

Schindler, D. W. and W. F. Donahue. 2006. An impending water crisis in Canada's western prairie provinces. Proceedings of the National Academy of Sciences of the United States of America 103:7210-7216.

Stichling, W. and S. R. Blackwell. 1957. Drainage area as a hydrologic factor on the glaciated Canadian Prairies. In: General Assembly of Toronto. International Association of Hydological Sciences Publication 45.

SWA (Saskatchewan Watershed Authority) 2008. Methodology to assess the water volume impact of wetland drainage in the Waldsea, Deadmoose, Houghton, and Fishing lake watersheds. Saskatchewan Government, Saskatchewan Watershed Authority, Regina, Saskatchewan, Canada.

Taube, C. M. 2000. Three methods for computing the volume of a lake. Chapter 12 *in* Schneider, J.C. 2000. Manual of fisheries methods II: with periodic updates. Michigan Department of Natural Resources, Fisheries Special Report 25, Ann Arbor.

Töyrä, J. A., A. Pietroniro, C. Hopkinson, and W. Kalbfleisch. 2003. Assessment of airborne scanning laser altimetry (lidar) in a deltaic wetland environment. Canadian Journal of Remote Sensing 29:718-728.

Töyrä, J. A., A. Pietroniro. 2005. Towards operational monitoring of a northern wetland using geomatics-based techniques. Remote Sensing of Environment 97:174-191.

Töyrä, J., A. Pietroniro, M. Craymer, and M. Veronneau. 2006. Evaluation of LiDAR-derived ground surface digital elevation model (DEM) in low-relief regions: case study on the Canadian prairies. In: Hydroscan: Airborne laser mapping of hydrological features and resources. Edited by: Chris Hopkins, Alain Pietroniro and John Pomeroy. Papers presented at: Hydroscan Conference, 22 September 2006, Saskatoon, Saskatchewan.

Ullah, W. and W. T. Dickinson. 1979. Quantitative description of depression storage using a digital surface model, II. Characteristics of surface depressions. Journal of Hydrology 42:77-90.

van der Kamp, G. and M. Hayashi. 1998. The groundwater recharge function of small wetlands in the semi-arid northern prairies. Great Plains Research 8:39-56.

van der Kamp, G., W. J. Stolte, and R. G. Clark. 1999. Drying out of small prairie wetlands after conversion of their catchments from cultivation to permanent brome grass. Hydrological Sciences Journal 44:387-397.

van der Kamp, G., M. Hayashi, and D. Gallen. 2003. Comparing the hydrology of grassed and cultivated catchments in the semi-arid Canadian prairies. Hydrological Processes 17:559-575.

van der Kamp, G. and M. Hayashi. 2009. Groundwater-wetland ecosystem interaction in the semiarid glaciated plains of North America. Hydrogeology Journal 17:203-214.

van der Valk, A. G. (ed.). 1989. Northern Prairie Wetlands. Iowa State University Press, Ames, IA, USA.

van der Valk, A, G. 2005. Water-level fluctuations in North American prairie wetlands. Hydrobiologia 539:171-188.

Vinning, K. C. 2002. Simulation of streamflow and wetland storage, Starkweather coulee subbasin, North Dakota, Water Years 1981-98. U.S. Geological Survey, U.S. Department of the Interior, Reston, Virginia, USA. Water-Resources Investigation Report 02-4113.

Voldseth, R. A., W. C. Johnson, T. Gilmanov, G. R. Guntenspergen, and B. V. Millett. 2007. Model estimation of land-use effects on water levels of northern prairie wetlands. Ecological Applications 17:527-540.

Warner, B.C. and C. D. A. Rubec. 1997. The Canadian wetlands classification system. 2nd revised edition. Wetlands Research Centre, University of Waterloo. 95 pp.

Waiser, M. 2006. Relationship between hydrological characteristics and dissolved organic carbon concentrations and mass in northern prairie wetlands using a conservative tracer approach. Journal of Geophysical Research 111:G02024, doi:10.1029/2005JG000088.

Wang, X., W. Yang, and A. M. Melesse. 2008. Using hydrologic equivalent wetland concept within SWAT to estimate streamflow in watersheds with numerous wetlands. Transactions of the American Society of Agricultural and Biological Engineers 51:55-72.

Whigham, D. F. and T. E. Jordan. 2003. Isolated wetlands and water quality. Wetlands 23:541-549.

Wiens, L. 2001. Surface area-volume relationships for prairie wetlands in the upper Assiniboine river basin, Saskatchewan. Canadian Water Resources Journal 26:503-513.

Winter, T. C., R. D. Benson, R. A. Engberg, G. J. Wiche, D. G. Emerson, O. A. Crosby, and J. E. Miller. 1984. Synopsis of ground-water and surface-water resources of North Dakota. U.S. Geological Survey Open-File Report 84-732. 127 pp.

Winter, T. C., and D. O. Rosenberry. 1995. The interaction of ground water with prairie pothole wetlands in the cottonwood lake area, east-central North Dakota, 1979-1990. Wetlands 15:193-211.

Winter, T. C. and D. O. Rosenberry. 1998. Hydrology of prairie pothole wetlands during drought and deluge: A 17-year study of the Cottonwood Lake wetland complex in North Dakota in the perspective of linger term measured and proxy hydrological records. Climatic Change 40:189-209.

Winter, T. C. and J. W. LaBaugh. 2003. Hydrologic considerations in defining isolated wetlands. Wetlands 23:532-540.

Woo, M. K. and R. D. Rowsell. 1993. Hydrology of a prairie slough. Journal of Hydrology 146:175-207.

Zimmerman, D., C. Pavlik, A. Ruggles, and M. P. Armstrong. 1999. An experimental comparison of ordinary and universal kriging and inverse distance weighting. Mathematical Geology 31:376-390.

APPENDIX A – DERIVING THE SHAPE INDEX

The shape index (SI) is based on comparing the perimeter (*P*) and area (*A*) of a wetland to the perimeter (i.e., circumference) and area of a circle. When quantifying and comparing the shape of a wetland or circle the perimeter cannot be simply divided by area because the SI value would decrease as the size of the wetland (or circle) increases (Figure A.1).

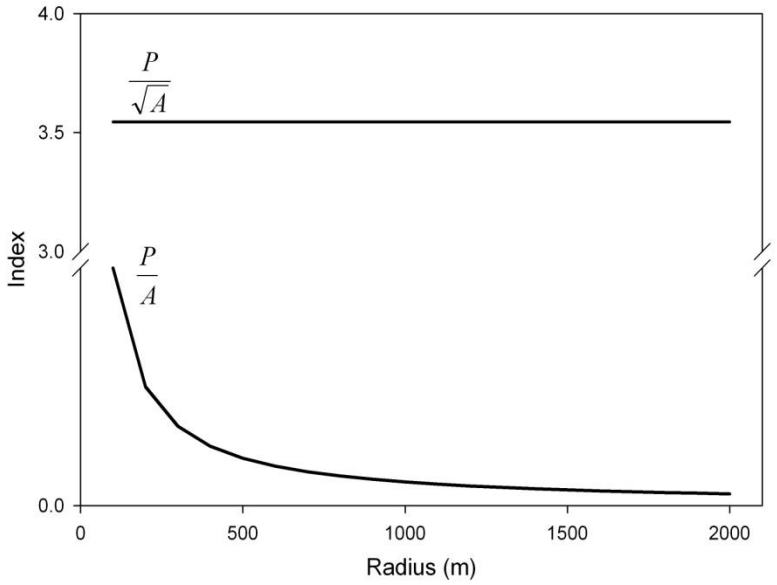

Figure A.1. Illustration of how two different shape indices vary with wetland radius.

However, by taking the square root of area SI values can be compared for different sized circles (i.e., wetlands) through

$$SI = \frac{P}{\sqrt{A}} \qquad \text{(A.1)}$$

For this research, wetland perimeters were compared to the perimeter of a circle with the same area (Forman and Godron 1986). The SI presented by McGarigal and Marks (1995) accomplished this by defining the perimeter-area relationship of a wetland (A.1) and circle (A.5), then combining them to derive the SI (A.8).

The SI of a circle is characterized by the relationship between perimeter

$$P = 2\pi r \tag{A.2}$$

and area

$$A = \pi r^2 \tag{A.3}$$

Inserting these terms into Eq. A.1 gives the SI of circle

$$SI = \frac{2\pi r}{\sqrt{\pi r^2}} \tag{A.4}$$

which can be simplified to

$$SI = 2\sqrt{\pi} \tag{A.5}$$

When comparing a perfectly circular wetland to a circle that has the same area, the perimeter-area relationship of the wetland (A.1) is equal to the perimeter-area relationship of the circle (A.5)

$$\frac{P}{\sqrt{A}} = 2\sqrt{\pi} \qquad \text{(A.6)}$$

Combining the above equation gives

$$\frac{P}{2\sqrt{\pi A}} = 1 \qquad \text{(A.7)}$$

where SI = 1 for a perfectly circular wetland. While natural wetlands may be very similar to a circle (e.g., SI = 1.01), they will never be a perfect euclidean circle. Therefore the SI of a natural wetland will always be greater than one. This SI relationship for wetlands was presented by McGarigal and Marks (1995) and is given through

$$\frac{P}{2\sqrt{\pi A}} > 1 \qquad \text{(A.8)}$$

APPENDIX B – DERIVING THE EQUATION FOR ESTIMATING WETLAND DEPTH

Since the LiDAR pulse is transmitted in the near-infrared, the DEM does not provide information on the depth of water (h_1) when the data were acquired (Figure B.1).

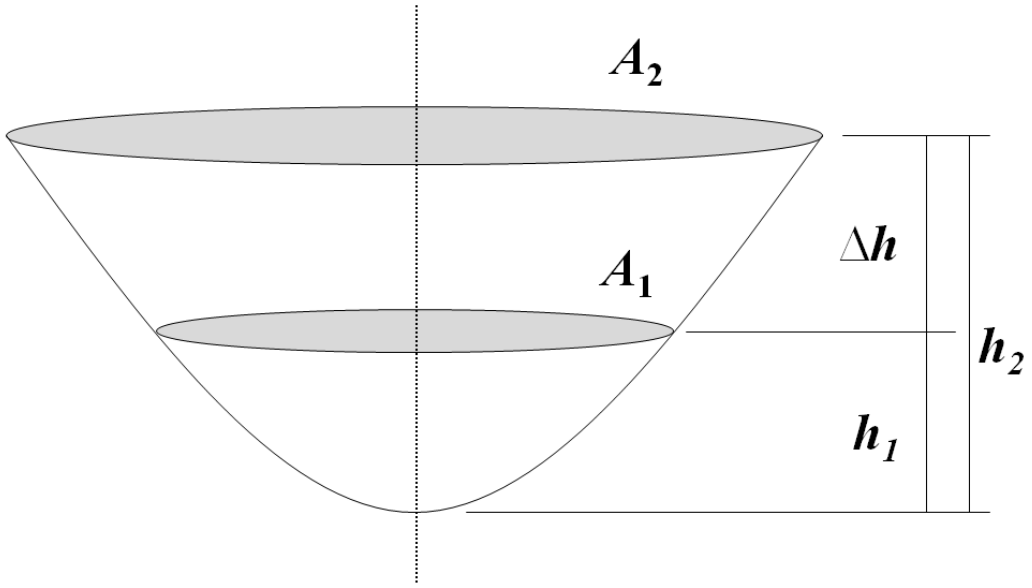

Figure B.1. Theoretical wetland illustrating area and depth measurements required to estimate the wetland depth from a LiDAR DEM.

However, through GIS analysis of the LiDAR DEM it is possible to measure A_1, A_2, and Δh. Since $\Delta h = h_2 - h_1$, the remaining measurement to measure is h_1. The Hayashi-van der Kamp equation for estimating area,

$$A = s\left(\frac{h}{h_o}\right)^{2/p} \qquad \text{(B.1)}$$

can be used to estimate the depth of water (h_1) when the LiDAR data were acquired if a constant p coefficient value is assumed.

The above equation can be rewritten to calculate A_1 through

$$A_1 = s\left(\frac{h_1}{h_o}\right)^{2/p} \quad \text{(B.2)}$$

provided that h_1, along with the s and p coefficient are known. Similarly, h_2 can be inserted into the above equation to calculate A_2. Therefore, the equation for A_2 can be divided by A_1 to give

$$\frac{A_2}{A_1} = \left(\frac{h_2}{h_1}\right)^{2/p} \quad \text{(B.3)}$$

Taking the reciprocal of the power isolates the depth measurements

$$\frac{h_2}{h_1} = \left(\frac{A_2}{A_1}\right)^{p/2} \quad \text{(B.4)}$$

This equation can be rewritten to solve for h_2 through

$$h_2 = \left(\frac{A_2}{A_1}\right)^{p/2} \times h_1 \quad \text{(B.5)}$$

However, since only Δh is known the above equation must be inserted into

$$\Delta h = h_2 - h_1 \tag{B.6}$$

to give

$$\Delta h = \left(\left(\frac{A_2}{A_1}\right)^{P/2} \times h_1\right) - h_1 \tag{B.7}$$

This equation can be rewritten to solve for h_1 through

$$h_1 = \frac{\Delta h}{(A_2/A_1)^{p/2}-1} \tag{B.8}$$

This equation calculates the depth of water at the time of LiDAR data acquisition (Figure B.1). Thus, this measurement of h_1 can be used to calculate the *s* coefficient (Eq. 2.6), or it can be added to Δh to calculate the depth of water when A_2 was measured (Figure B.1).

APPENDIX C – MAXIMUM VOLUME AND AREA FOR STUDY WETLANDS

Table C.1. Actual maximum volume and area for the study wetlands

Wetland ID	h_{max}(m)	A_{max}(m^2)	V_{max}(m^3)	Wetland ID	h_{max}(m)	A_{max}(m^2)	V_{max}(m^3)
Smith Creek				*St. Denis*			
B1	0.90	2980	1320	D1	0.30	660	80
W1	0.65	1770	520	D2	0.45	360	70
W2	0.60	5000	1420	D3	0.70	760	240
W3	0.50	2280	330	S1	2.65	67540	83640
W4	0.50	2210	470	S90	3.40	164340	347000
W7	0.50	1700	380	S92	1.20	3220	1710
W8	0.45	1120	210	S97	0.70	10590	4500
W9	0.70	7260	2540	S104	0.70	1260	430
W10	0.90	1800	670	S109	1.20	4140	2150
W11	0.45	2650	550	S120	1.10	3150	1880
LR2	0.50	3000	710	S124	0.60	1870	540
LR3	1.10	14060	7340	S125n&s	1.80	21870	17840
LR4	0.85	3890	1400	S125s	1.35	5980	3760
LR7	0.75	11870	4710				

APPENDIX D – VISUAL BASIC CODE

```
Sub Batch_LiDAR_Analysis()

    ' (comment about code) Saves the name of the wookbook that will be opened
    Dim WB_To_Open As String

     'This collects the name of the first workbook in this folder (the folder that this spreadsheet is
      in)
     WB_To_Open =
      Dir(["C:\GIS_Data\LiDAR_Model_Output\SDNWA\SDNWA_Output\dBase\"] & "*.dbf")

    'All of the code to process the data is contained in a Do While loop
    'The Do While loop cycles through all of the files in the current folder
     Do While WB_To_Open <> ""
        Workbooks.Open
     Filename:="C:\GIS_Data\LiDAR_Model_Output\SDNWA\SDNWA_Output\dBase\" &
     WB_To_Open

       'BEGIN LIDAR ANALYSIS CODE

       'This section sorts the data from largest to smallest based on the area
       Columns("A:D").Select
       ActiveWorkbook.ActiveSheet.Sort.SortFields.Clear
       ActiveWorkbook.ActiveSheet.Sort.SortFields.Add Key _
          :=Range("D2:D6500"), SortOn:=xlSortOnValues, Order:=xlDescending, _
          DataOption:=xlSortNormal
       With ActiveWorkbook.ActiveSheet.Sort
          .SetRange Range("A1:D6500")
          .Header = xlYes
          .MatchCase = False
          .Orientation = xlTopToBottom
          .SortMethod = xlPinYin
          .Apply
       End With

       'This section deletes the ArcGIS columns not needed. Keeps elevation and area
       Columns("A:A").Select
       Selection.delete Shift:=xlToLeft
       Columns("B:B").Select
       Selection.delete Shift:=xlToLeft

       'This code collects the maximum area for future calculations
       maxA = Cells(2, 2).Value
```

```
'This section sets variables
 n = 1   'counter
 X = 2   'counter
 Dim a As Double

  'This code asks for user input. The goal is to determine which area measurements are not
   desired
a = InputBox(Prompt:="What is the smallest surface area you would like to keep?")
'This is blanked out temporarily. Can be used as a constant 'a = 2

'This code determines how many area measurements there are
AreaCount = WorksheetFunction.CountA(Range("A2:A6500"))

'This section keeps the desired area measurements and erases the rest
Do While n <= AreaCount
    If Cells(X, 2).Value < (a - 0.00001) Then
    Cells(X, 1).Value = Null
    Cells(X, 2).Value = Null
    End If

X = X + 1
n = n + 1

Loop

'This section sorts the data from smallest to largest based on the area
Columns("A:B").Select
ActiveWorkbook.ActiveSheet.Sort.SortFields.Clear
ActiveWorkbook.ActiveSheet.Sort.SortFields.Add Key:=Range("A1"), _
    SortOn:=xlSortOnValues, Order:=xlAscending, DataOption:=xlSortNormal
With ActiveWorkbook.ActiveSheet.Sort
    .SetRange Range("A1:B6500")
    .Header = xlYes
    .MatchCase = False
    .Orientation = xlTopToBottom
    .SortMethod = xlPinYin
    .Apply
End With

'This section sets the number of decimals for the elevation and area measurements
Range("A2").Select
Range(Selection, Selection.End(xlDown)).Select
Selection.NumberFormat = "0.000"

Range("B2").Select
Range(Selection, Selection.End(xlDown)).Select
```

```
Selection.NumberFormat = "0.000"

Dim count As Double

Dim combo As Double

count = WorksheetFunction.CountA(Range("A2:A25"))
'determines how many area measurements there are

n = Application.WorksheetFunction.Combin(count, 2)
'determines the possible number of combinations
'based on the number of area measurements

combo = count   'counts the number of combinations
 combo2 = count  'also counts the number of combinations but different variable because
    the orginal should not be changed

'The next few sections determines all of the possible combinations based on the number of
   area measurements.
 'The next few sections makes seven new columns of data with the combinations, delta h,
    and s values
X = 2   'Row number for E1, A1, E2, A2
w = 3   'Row number for Elevation 1 and Area 1
q = 2   'Row number for Elevation 2 and Area 2
a = w   'Facilitates correct row number for E1, A1
b = 1   'Counts the number of combinations produced
d = 1   'Facilitates the # combos per group
'This code asks for the user to input the p basin shape coefficient value.
p = InputBox(Prompt:="Enter the Hayashi-van der Kamp p coefficient")

'This section inserts the column titles
Cells(1, 3) = "Elevation 1 (m)"
Cells(1, 4) = "Area 1 (m2)"
Cells(1, 5) = "Elevation 2 (m)"
Cells(1, 6) = "Area 2 (m2)"
Cells(1, 7) = "Delta h (m)"
Cells(1, 8) = "Depth to Area1 (m)"
Cells(1, 9) = "s coefficient (m2)"

'This is the code that loops through the area and elevation data to make the combinations
'This code also calculates delta h, the depth to area 1, and the s coefficients
Do While b <= n
  Do While d < combo
      Cells(X, 3).Value = Cells(w, 1).Value
      Cells(X, 4).Value = Cells(w, 2).Value
      Cells(X, 5).Value = Cells(q, 1).Value
```

```
        Cells(X, 6).Value = Cells(q, 2).Value
        Cells(X, 7).Value = Cells(X, 3).Value - Cells(X, 5).Value
        Cells(X, 8).Value = Cells(X, 7).Value + (Cells(X, 7).Value / (((Cells(X, 4).Value /
              Cells(X, 6).Value) ^ (p / 2)) - 1))
        Cells(X, 9).Value = Cells(X, 4).Value / (Cells(X, 8).Value ^ (2 / p))
        X = X + 1
        w = w + 1
        b = b + 1
        d = d + 1
    Loop

    d = 1
    q = q + 1
    w = (combo2 + 1) - (combo2 - a)
    a = a + 1
    combo = combo - 1
Loop

'This code calculates the average s coefficient
Cells(1, 10) = "average s coefficient (m2)"
Cells(2, 10) = WorksheetFunction.average(Range("I2:I6500"))

'The follow section formats the number of decimal places for the column with elevation 1
     data
Range("C2").Select
Range(Selection, Selection.End(xlDown)).Select
Selection.NumberFormat = "0.000"

'The follow section formats the number of decimal places for the column with area 1 data
Range("D2").Select
Range(Selection, Selection.End(xlDown)).Select
Selection.NumberFormat = "0.000"

'The follow section formats the number of decimal places for the column with elevation 2
     data
Range("E2").Select
Range(Selection, Selection.End(xlDown)).Select
Selection.NumberFormat = "0.000"

'The follow section formats the number of decimal places for the column with area 2 data
Range("F2").Select
Range(Selection, Selection.End(xlDown)).Select
Selection.NumberFormat = "0.000"

'The follow section formats the number of decimal places for the column with delta h data
Range("G2").Select
```

```
Range(Selection, Selection.End(xlDown)).Select
Selection.NumberFormat = "0.000"

'The follow section formats the number of decimal places for the column with depth to area
    1 data
Range("H2").Select
Range(Selection, Selection.End(xlDown)).Select
Selection.NumberFormat = "0.000"

'The follow section formats the number of decimal places for the column with the s value
    data
Range("I2").Select
Range(Selection, Selection.End(xlDown)).Select
Selection.NumberFormat = "0.000"

'The follow section formats the number of decimal places for the column with the average s
    value
Range("J2").Select
Range(Selection, Selection.End(xlDown)).Select
Selection.NumberFormat = "0.000"

'This section makes the column width fi the data
Columns("A:J").EntireColumn.AutoFit

'This section centres the elevation and area data in column A and B
Range("A1:B1").Select
Range(Selection, Selection.End(xlDown)).Select
With Selection
   .HorizontalAlignment = xlCenter
   .VerticalAlignment = xlBottom
   .WrapText = False
   .Orientation = 0
   .AddIndent = False
   .IndentLevel = 0
   .ShrinkToFit = False
   .ReadingOrder = xlContext
   .MergeCells = False
End With

'This section centres the data in column C to I
Range("C1:I1").Select
Range(Selection, Selection.End(xlDown)).Select
With Selection
   .HorizontalAlignment = xlCenter
   .VerticalAlignment = xlBottom
   .WrapText = False
```

```
    .Orientation = 0
    .AddIndent = False
    .IndentLevel = 0
    .ShrinkToFit = False
    .ReadingOrder = xlContext
    .MergeCells = False
End With

'This section centres the data in column J
Range("J1:J1").Select
Range(Selection, Selection.End(xlDown)).Select
With Selection
    .HorizontalAlignment = xlCenter
    .VerticalAlignment = xlBottom
    .WrapText = False
    .Orientation = 0
    .AddIndent = False
    .IndentLevel = 0
    .ShrinkToFit = False
    .ReadingOrder = xlContext
    .MergeCells = False
End With

'This section lists the depth values in meters
Dim h As Double
'This code calculates the maximum depth of the wetland based on the maximum surface
      area
'The maximum depth is calculated by rearranging Eq. 3 (Hayashi and van der Kamp 2000)
maxH = (maxA / Cells(2, 10).Value) ^ (0.5 * p)

Hvalue = 0.1
r = 2
'This code writes the column titles
Cells(1, 12).Value = "Depth (m)"
Cells(1, 13).Value = "Area (m2)"
Cells(1, 14).Value = "Volume (m3)"
'This loop calculates the depth up to the user input hmax
'This loop calculates the area and volume using the Hayashi-van der Kamp V-A-h
      equations.
'The p coefficient value is constant and was input earlier in the code
'The s coefficient value used is the average of the combination analysis
Do While Hvalue <= (maxH)
    Cells(r, 12).Value = Hvalue
    Cells(r, 13).Value = Cells(2, 10).Value * ((Cells(r, 12).Value / 1) ^ (2 / p))
    Cells(r, 14).Value = (Cells(2, 10).Value / (1 + (2 / p))) * ((Cells(r, 12).Value ^ (1 + (2 /
      p))) / (1 ^ (2 / p)))
```

```
    Hvalue = Hvalue + 0.05
    r = r + 1
Loop

'This section adds an additional row to the area and volume columns
'The code inserts in the maximum depth, based on the maximum contour area
'The code inserts the area and volume based on the maximum depth
Cells(r, 12).Value = maxH
Cells(r, 13).Value = Cells(2, 10).Value * ((maxH / 1) ^ (2 / p))
Cells(r, 14).Value = (Cells(2, 10).Value / (1 + (2 / p))) * ((maxH ^ (1 + (2 / p))) / (1 ^ (2 /
    p)))

'This section sets the decimnal places for the depth column
Range("L2").Select
Range(Selection, Selection.End(xlDown)).Select
Selection.NumberFormat = "0.000"

'This section sets the decimnal places for the estimated area column
Range("M2").Select
Range(Selection, Selection.End(xlDown)).Select
Selection.NumberFormat = "0.000"

'This section sets the decimnal places for the estimated volume column
Range("N2").Select
Range(Selection, Selection.End(xlDown)).Select
Selection.NumberFormat = "0.000"

'This section aligns the depth, area and volume data in the centre of the column
Range("L1:N1").Select
Range(Selection, Selection.End(xlDown)).Select
With Selection
    .HorizontalAlignment = xlCenter
    .VerticalAlignment = xlBottom
    .WrapText = False
    .Orientation = 0
    .AddIndent = False
    .IndentLevel = 0
    .ShrinkToFit = False
    .ReadingOrder = xlContext
    .MergeCells = False
End With

'This section makes the width of the column fit the data
Columns("L:N").EntireColumn.AutoFit

'END LIDAR ANALYSIS CODE
```

```
        'This section of the Do While loop closes the open spreadsheet and asks to save it
        Workbooks(WB_To_Open).Close
        'This code updates the wookbook to open by selecting the next spreadsheet in the folder
        WB_To_Open = Dir()
    Loop

End Sub
```